

MICROBIAL STRATIFICATION AND INFERRED MICROBIALLY CATALYZED PROCESSES
ALONG A DEEP-SEA HYPERSALINE CHEMOCLINE

Andrew Hyde

A thesis submitted to the faculty at the University of North Carolina at Chapel Hill in partial fulfillment of the requirements for the degree of Master of Science in the Department of Marine Sciences in the College of Arts and Sciences.

Chapel Hill
2018

Approved by:

Andreas P. Teske

Carol Arnosti

Marc J. Alperin

©2018
Andrew Hyde
ALL RIGHTS RESERVED

ABSTRACT

Andrew Hyde: Microbial stratification and microbially catalyzed processes along a deep-sea hypersaline chemocline
(Under the direction of Andreas Teske)

The Gulf of Mexico contains the world's largest anoxic hypersaline seafloor basin, Orca Basin. The water contained in this 400 km² bathymetric depression is roughly eight times as saline as the overlying seawater. The resulting density contrast prevents the 200 m deep brine layer from mixing with seawater, creating an interface that traps particles of organic matter falling through the water column. The concentrated organic matter at the interface is hypothesized to host a thriving bacterial community that has yet to be characterized. Here, I present the results of the first bacterial community analysis by high-throughput sequencing ever conducted on the interface and brine pool of Orca Basin. I discuss how the bacterial community changes along a 550 m vertical transect with regards to oxygen, salinity, and organic matter gradients. Finally, a comparison of the geochemical and bacterial composition of Orca Basin to brine pools in the Mediterranean and Red Seas reveals the uniqueness of Orca Basin in a global context. This research adds to our current knowledge of biodiversity in global hypersaline habitats and has implications for our understanding of sulfur and carbon cycling in extreme environments.

TABLE OF CONTENTS

LIST OF FIGURES	vi
LIST OF TABLES.....	vii
LIST OF ABBREVIATIONS	viii
1 INTRODUCTION.....	1
1.1 ORIGINS OF DHABS IN THE MEDITERRANEAN AND RED SEAS	2
1.2 ORIGINS OF DHABS IN THE GULF OF MEXICO	3
1.3 MICROBIAL LIFE IN DHABS	5
2 MATERIALS AND METHODS.....	8
2.1 SAMPLING AND DNA EXTRACTIONS.....	8
2.2 SEQUENCING	8
2.3 DATA ANALYSIS	9
2.3.1 <i>Orca Basin</i>	9
2.3.2 <i>Other DHABs</i>	11
3 RESULTS.....	13
3.1 WHOLE BACTERIAL COMMUNITY	13
3.2 A-DIVERSITY.....	14
3.3 B-DIVERSITY.....	16
3.4 EXAMINATION OF SPECIFIC CLADES	19

3.4.1	<i>Marinimicrobia</i> (SAR406, Marine Group A)	19
3.4.2	<i>Alphaproteobacteria</i>	22
3.4.3	<i>Gammaproteobacteria</i>	22
3.4.4	<i>Deltaproteobacteria</i>	24
3.4.5	<i>Actinobacteria</i>	25
3.4.6	<i>MSBL2</i>	26
3.5	MEDITERRANEAN AND RED SEA DHABS	27
4	DISCUSSION	32
4.1	SULFUR CYCLING IN THE ORCA BASIN CHEMOCLINE	32
4.2	CARBON METABOLISM IN THE ORCA BASIN CHEMOCLINE	34
4.3	COMPARISON OF ORCA BASIN TO OTHER DHABS	36
	REFERENCES	39

LIST OF FIGURES

<i>Figure 1</i>	<i>Map of sampling location in the Gulf of Mexico.....</i>	<i>8</i>
<i>Figure 2</i>	<i>Class-level bacterial community composition for Orca Basin.....</i>	<i>14</i>
<i>Figure 3</i>	<i>Measures of alpha-diversity in the Orca Basin chemocline.....</i>	<i>16</i>
<i>Figure 4</i>	<i>Principle Coordinate analyses).....</i>	<i>18</i>
<i>Figure 5</i>	<i>Distribution of Marinimicrobia along the Orca Basin halocline</i>	<i>19</i>
<i>Figure 6</i>	<i>Phylogenetic placement of OTU1216.....</i>	<i>21</i>
<i>Figure 7</i>	<i>Distribution of Alphaproteobacteria along the Orca Basin halocline.....</i>	<i>22</i>
<i>Figure 8</i>	<i>Distribution of Gammaproteobacteria along the Orca Basin halocline.....</i>	<i>23</i>
<i>Figure 9</i>	<i>Distribution of Deltaproteobacteria along the Orca Basin halocline</i>	<i>24</i>
<i>Figure 10</i>	<i>PCoA analysis on the Deltaproteobacterial community.....</i>	<i>25</i>
<i>Figure 11</i>	<i>Distribution of Actinobacteria along the Orca Basin halocline</i>	<i>26</i>
<i>Figure 12</i>	<i>Distribution of WWE1 phylum along the Orca Basin halocline</i>	<i>27</i>
<i>Figure 13</i>	<i>Comparison of the interface bacterial communities of the different DHABs.....</i>	<i>28</i>
<i>Figure 14</i>	<i>Comparison of bacterial communities in different brine pools.....</i>	<i>29</i>
<i>Figure 15</i>	<i>Comparison of the Deltaproteobacteria in different DHAB interfaces and gradients.....</i>	<i>30</i>

LIST OF TABLES

Table I. Geochemical properties of global DHABs compiled from literature. 7

*Table II. Available sequence data from other brine pools
in the Mediterranean and Red Sea..... 12*

LIST OF ABBREVIATIONS

DHAB	Deep hypersaline anoxic basin
MSBL2	Mediterranean Sea Brine Lake (group) 2
Myr	Million years
OTU	Operational taxonomic unit
PCoA	Principle coordinate analysis

1 *Introduction*

Deep hypersaline anoxic basins (DHABs) are some of the harshest environments on Earth. These otherworldly hydrographic features present numerous challenges to life, such as extreme salinities (over 500 g/L in some cases), high pressures, elevated temperatures, and high concentrations of sulfides or heavy metals. First discovered in 1946-7 by the Swedish R/V *Albatross* in the Red Sea¹, this “abnormal water” has since been found in the Mediterranean Sea and the Gulf of Mexico. The limited extent of this phenomenon is owed to the unique set of geological features that must be present for the formation of DHABs: namely, the formation of an evaporite layer and its subsequent dissolution.

Underneath each DHAB lies a thick layer of salt, serving as the source for the hypersaline water found in these deep sea brine pools. The particulars of how these extensive salt deposits formed vary by site, but the main principle is the same. When seawater evaporates, it leaves behind the dissolved ions, which subsequently form solids (“salt”) in a characteristic order. When 50% of the seawater has evaporated, carbonate minerals (e.g. CaCO_3) precipitate out of solution. At 80% water loss, gypsum (CaSO_4) precipitates, followed by halite (NaCl) at 90% water loss². Lastly, K-Mg salts will only precipitate when only 2% of the original volume of seawater remains².

This happens on oceanic scales when a body of water is isolated from other water bodies, leading the formation of an evaporative basin. Sedimentation covers these evaporative layers, and when a new input of water arrives (due to a change in geologic conditions), the evaporite layers remain buried under the new sediment-seawater interface.

1.1 Origins of DHABs in the Mediterranean and Red Seas

The evaporites in the Red and the Mediterranean Seas were formed in the late Miocene (~5-8 Myr) when these two bodies of water were connected^{3,4}. During this so-called “Messinian Salinity Crisis”, the oceanic connection between the Mediterranean/Red Sea and the Atlantic Ocean was severed, forming an evaporative basin. The exact mechanism behind the closing of the Strait of Gibraltar is unresolved and was originally attributed to eustatic sea-level fall due to glaciation⁵. More recent work has proposed that the closing of the Mediterranean-Atlantic gateway was caused by magmatic intrusions and asthenospheric upwelling along the Iberian and African margins^{6,7}. Evidence supporting this hypothesis comes from changes in igneous geochemistry from this time period as well as thermochemical modeling⁶.

Once these salt layers are buried, they may remain undisturbed unless other geological processes act to expose them in some manner. While the origins of the salt deposits in the Mediterranean and Red Seas are the same, the subsequent processes that have exposed them are very different.

All of the DHABs in the Mediterranean Sea are located in the eastern region along a structure called the Mediterranean Ridge⁸. Here, the African plate is subducting underneath the Eurasian and Anatolian plates; this subduction exposes the

1.5-km thick⁷ Messinian evaporites to ambient seawater, thus initiating their local dissolution. If this occurs near a bathymetric depression in the sediment, the highly dense brine collects in a brine pool and does not mix with the overlying water column⁸. Most DHABs are dominated by Na⁺ and Cl⁻, as they are fueled largely by halite (see Table I). However, a few DHABs in the eastern Mediterranean (e.g. Discovery and Kryos Basin) are instead formed as later stage evaporites (e.g. bischofite, [(MgCl₂) 6H₂O]) are exposed and dissolved to form brine water^{2,9,10}. This is possibly due to the extent of evaporation during the Messinian Salinity Crisis^{6,7}, since Mg-based salts only theoretically precipitate under extreme evaporative events (see above)².

The Messinian salt deposits in the Red Sea share an origin with those in the Mediterranean Sea since the two were connected during the Miocene epoch³. The tectonic processes that expose the evaporites differ significantly between the two seas. While the Mediterranean DHABs owe their existence to tectonic subduction, the evaporites in the Red Sea are exposed by an active spreading center at the African-Arab plate boundary^{4,11-13}. There is not one mechanism that explains the formation of the more than 25 DHABs in the Red Sea¹⁴; however, in general, hydrothermal influence of the spreading center results in very hot (Atlantis II Deep is currently 71 °C and rising), metal-rich, sulfidic brine waters^{11,12,14}.

1.2 Origins of DHABs in the Gulf of Mexico

The Gulf of Mexico is the only other place on Earth we have discovered DHABs¹⁵, providing a valuable site to compare the Red and Mediterranean DHABs to. It is also the location where the largest DHAB is found, Orca Basin (400 km²)¹⁵. Given its

geographic distance from the Red and Mediterranean Seas, it perhaps not surprising that the source of salt for Orca Basin is different than other DHABs. Instead of the late Miocene (~5.5 myr⁶) era deposits, Orca Basin is fed by a far more ancient mid-Jurassic (Callovian, ~165 myr) salt deposit, the “Louann salt”¹⁶. The 3-4 km thick Louann salt was deposited as parts of the Gulf of Mexico were isolated from the nascent Atlantic Ocean, forming an evaporite basin in a similar fashion to the Messinian Salinity Crisis^{16,17}. Subsequent sedimentation and a re-flooding of the Gulf lead to the burial of the world’s largest salt deposit^{16,17}.

In the Mediterranean and Red Seas, the salt deposits are exposed via active tectonic processes (subduction in the Eastern Mediterranean and rifting in the Red Sea). However, the Louann salt deposit is exposed through a process called salt tectonics^{16,17}. Newly deposited sediment puts more pressure on the sediment below it; as the pressure increases, the sediment is “de-watered”, forcing the porewater upwards and thereby increasing the density of the sediment to approx. 2.6-2.8 g/cm³ (°). The Louann salt deposit has a density of approximately 2.2 g/cm³ and therefore rises in the sediment column until it achieves neutral buoyancy⁹.

In some areas of the Gulf of Mexico, these salt diapirs get very close to the sediment-water interface and may even be exposed to ambient seawater¹⁸. One of these outcroppings happens to be adjacent to a bathymetric depression in the northern Gulf of Mexico. As seawater laterally advects over this exposed salt, the subsequent increase in density causes the newly formed brine water to sink into the basin. This is in contrast to the Mediterranean and Red Sea DHABs, which have salt sources beneath the basin (see above). It is thought that this process has been

happening in Orca Basin for ~8000 years¹⁹, resulting in a current brine volume of 13.3 km³. Orca Basin is divided into two lobes or sub-basins: a northern and a southern basin separated by a shallower, more narrow saddle (see Figure 1).

1.3 Microbial life in DHABs

Salt presents one of the harshest constraints on microbial life by increasing the osmotic pressure on a cell as well as decreasing the water activity²⁰. Some DHABs have total salinities of 510 g/kg H₂O, which reduces the activity of water to 0.382, which is near the theoretical lower limit for known life¹⁰. Despite these hostile conditions, life persists in DHABs, as revealed by monitoring primary productivity²¹, qPCR²², and metatranscriptomic studies²³.

The interfaces of these DHABs also serve as an interesting habitat for any potential inhabitants by trapping organic matter that falls through the water column once the density of the particle is matched by the density of the fluid. These “particle traps” are rich in organic matter and provide a unique microbial niche above the brine pool. In the case of Orca Basin, the concentration of DOC was shown to be 0.3 mM at the interface, compared to >0.1 mM in the overlying water column²⁴. Further work utilizing $\delta^{13}\text{C}$ and box models indicated the isotopically light DIC pool at the interface ($\delta^{13}\text{C}$ -20‰ compared to $\delta^{13}\text{C}$ 0‰ in the overlying seawater) was likely due to the remineralization of organic matter at the interface¹⁹. No further work has been published on this problem.

The metabolism and identities of microbial life in Mediterranean and Red Sea DHABs has been fairly well characterized^{10,22,23,25-43}, but published microbial studies on Orca Basin are limited^{19,44-47} and no bacterial community sequence data from the

water column or brine pool are publically available. Here we present the first characterization of Orca Basin's bacterial community.

	Temp (°C)	Salinity (g/L)	Na+ (mM)	Cl- (mM)	Mg2+ (mM)	K+ (mM)	Ca2+ (mM)	SO42- (mM)	HS- (mM)	Br- (mM)	NH4+ (mM)	CH4 (mM)	Max brine depth (m)	Interface thickness (m)	Sources
<i>Discovery</i>	14.5	510	68	9491	4995	19.6	2.6	96	0.7	N.D.	N.D.	0.031	60	N.D.	van der Wielen et al, 2005; Yakimov et al 2014
<i>Kryos</i>	14.5	471	125	9043	4379	80	1	320	N.D.	N.D.	N.D.	N.D.	160	2.5	Yakimov et al, 2014
<i>Thetis</i>	15.06	348	4760	5300	604	230	9	265	2.12	6	2.75	N.D.	N.D.	1	La Cono et al, 2011
<i>L'Atalante</i>	14.34	352	4670	5290	533	300	5.9	323	2.9	5	2.87	0.52	60	1.5	La Cono et al, 2011; van der Wielen et al, 2005
<i>Bannock</i>	15.12	323	4200	5380	644	127	16.3	135	2.9	9	3.35	0.45	500	N.D.	La Cono et al, 2011; van der Wielen et al, 2005
<i>Tyro</i>	14.17	321	5300	5350	71.1	19.2	35.4	52.7	2.1	1.28	1.3	N.D.	N.D.	N.D.	La Cono et al, 2011
<i>Urania</i>	18.32	240	3505	3730	315	122	31.6	107	15	9	2.87	5.56	200	N.D.	La Cono et al, 2011
<i>Medee</i>	15.44	345	4178	5259	788	471	2.8	201	1.64	65.3	2.35	0.0139	N.D.	50	Yakimov et al, 2013
<i>Atlantis II Deep</i>	67.8	262	4900	5200	29.1	63.2	142.2	8.3	N.D.	1.5	0.806	N.D.	N.D.	4	Ngugi et al, 2015
<i>Discovery Deep</i>	44.8	260	4700	5100	33	60.8	134.1	8.4	N.D.	1.5	0.852	N.D.	N.D.	35	Ngugi et al, 2015
<i>Erba Deep</i>	28.2	181	3200	3300	71.4	34.5	32.7	41.6	N.D.	1.4	0.691	N.D.	N.D.	10	Ngugi et al, 2015
<i>Kebrit Deep</i>	23.4	260	4800	5000	118.7	35.5	53.6	27.7	N.D.	3	2.657	N.D.	N.D.	3	Ngugi et al, 2015
<i>Nereus Deep</i>	30.1	224	3500	4200	67.4	71.4	224.7	10.5	N.D.	1.5	1.116	N.D.	N.D.	12	Ngugi et al, 2015
<i>GC233</i>	N.D.	121	1751	2092	9.7	22	36	1	N.D.	N.D.	11	N.D.	N.D.	N.D.	Joye et al, 2005
<i>GB425</i>	N.D.	130	1790	2114	8.7	89	59	1	N.D.	N.D.	7.6	N.D.	N.D.	N.D.	Joye et al, 2005
<i>Orca Basin</i>	5	250	4240	4450	42.4	17.2	29	20	N.D.	N.D.	0.5	N.D.	N.D.	80 m	Shokes et al, 1979 ; van Capellen et al, 1998; this

Table I. Geochemical properties of global DHABs compiled from literature.

2 Materials and methods

2.1 Sampling and DNA extractions

A CTD rosette sampler was deployed in Southern Orca Basin (26.91206, -91.37418) on 14 April 2014 from the R/V *Atlantis*. Twenty-three samples were taken at various depths (see figure) above, within, and below the halocline. On board, 700 mL water were filtered through 0.2 μm Millipore GTTP polycarbonate filters. The filtrate was discarded and filters were stored and transported at -80°C until DNA extraction in the home lab.

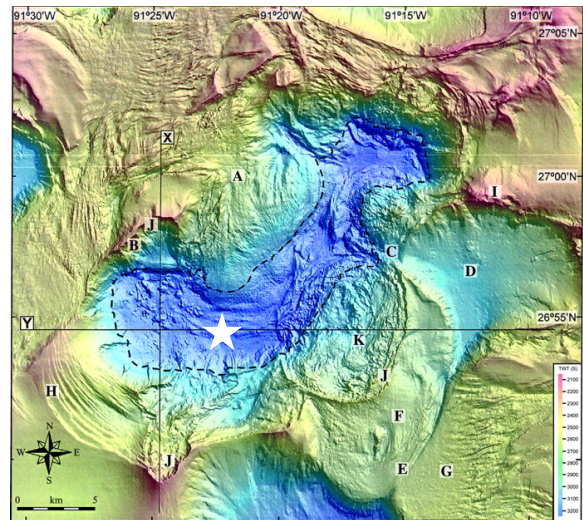


Figure 1 Map of sampling location in the Gulf of Mexico. The star indicates where the CTD was cast and samples collected (26.91206, -91.37418).

DNA was extracted from the filters using the MoBio PowerSoil Kit™ (Qiagen; Carlsbad, CA). PCR amplification and Nanodrop measurements were used to confirm the presence of DNA.

2.2 Sequencing

The V1-V2 region of the 16S rRNA gene was targeted using the PCR primers 8F (5'- GTTTGATCMTGGCTCAG-3') and 338R (3'-TGAGGATGCCCTCCGT-5')⁴⁸ and sequenced bidirectionally using the Illumina MiSeq platform at the University of Texas at Austin's Genomic Sequencing and Analysis Facility.

2.3 Data Analysis

2.3.1 Orca Basin

Forward and reverse reads were joined using SeqPrep⁴⁹. De novo operational taxonomic units (OTUs) were defined at 0.97 identity and picked using the UCLUST algorithm⁵⁰. One representative sequence was picked for each OTU using the default settings on QIIME⁵¹. Taxonomy was assigned to each representative sequence using four different reference databases: the Ribosomal Database Project (RDP)⁵², UCLUST⁵⁰, SortMeRNA⁵³, and mothur. RDP was able to assign taxonomic identity to the most sequences, and is therefore presented below. All singleton sequences were removed as well as all OTUs found in only one sample.

The representative sequences were aligned using PyNAST (Python Nearest Alignment Space Termination⁵⁴)- all unsuccessfully aligned sequences were removed. Chimera Slayer⁵⁵ was used to identify chimeric sequences, which were subsequently removed. Finally, a tree was constructed for all OTUs using FastTree2⁵⁶.

2.3.1.1 Statistical analyses

Samples were rarefied in PhyloSeq⁵⁷. All α -diversity analyses were carried out on the rarefied dataset; while β -diversity analyses were carried out on both a rarefied and unrarefied dataset⁵⁸.

α -diversity was calculated using three different metrics: OTU counts (accounts for richness), ACE richness (accounts for richness), and Shannon Diversity (accounts for richness and evenness).

$$S_{ACE} = S_{abund} + \frac{S_{rare}}{C_{ACE}} + \frac{F_1}{C_{ACE}} \gamma_{ACE}^2$$

Equation 1 . ACE diversity index-

ACE values were calculated using Equation 1. Where S_{abund} is the number of species observed more than ten times for a given sample, and S_{rare} the number of species observed less than ten times in a given sample⁵⁹.

Shannon-diversity indices were calculated using Equation 2⁶⁰. Where P_i is the fraction of the dataset the i^{th} OTU comprises. This frequency is multiplied by the natural log of itself and iterated for all OTUs.

$$H' = - \sum P_i \ln P_i$$

Equation 2. Shannon Diversity Index

For β -diversity, three different dissimilarity matrices were calculated for both the rarefied and unrarefied dataset: Weighted UniFrac, Unweighted UniFrac, and Bray-Curtis Dissimilarity.

$$u = \sum_i^n b_i \times \left| \frac{A_i}{A_T} - \frac{B_i}{B_T} \right|$$

Equation 3. Equation for Weighted Unifrac dissimilarity matrix calculations

The Weighted UniFrac dissimilarity matrix was calculated using Equation 3. Here, n is the number of branches in the phylogenetic tree provided, b_i is the length of branch i . A_i and B_i are the number of sequences that descend from the i^{th} branch for samples A and B. A_T and B_T are the total number of sequences in samples A and B⁶¹.

UniFrac (unweighted) calculations were done using Equation 4. Here, N is the number of nodes in the provided phylogenetic tree, l_i is the distance between node i and its parent node, and A_i and B_i are set to either 0 or 1 for absence or presence of a given node in samples A or B⁶².

$$u = \frac{\sum_{i=1}^N l_i |A_i - B_i|}{\sum_{i=1}^N l_i \max(A_i, B_i)}$$

Equation 4. Unweighted Unifrac calculation

The Bray-Curtis Dissimilarity matrix is calculated according to Equation 5.

Where A and B are communities and $S_{A,i}$ and $S_{B,i}$ are the number of individuals for the i^{th} OTU in communities A and B ⁶³.

$$D = 1 - 2 \frac{\sum \min(S_{A,i}, S_{B,i})}{\sum S_{A,i} + \sum S_{B,i}}$$

Equation 5. Bray-Curtis Dissimilarity formula

2.3.2 Other DHABs

DNA sequences were compiled from all papers written on DHABs that included 16S rRNA gene sequences from the GenBank database ⁶⁴ (Table II). Data analyses were conducted in the same manner as the Orca Basin sequences.

<i>Reference</i>	<i>Sites</i>	<i>Sequencing method</i>	<i>Nucleotide accession numbers</i>	<i>Number of sequences downloaded</i>
<i>van der Wielen et al, 2005</i>	L'Atalante (brine), Urania Basin (brine), Discovery Basin (brine and interface), Bannock Basin (brine)	full-length RT-PCR	AY226191:AY226381 (Bacteria)	150
<i>Borin et al, 2009</i>	Urania Basin (brine)	full-length RT-PCR	AY164322-AY164333 (Archaea); AY226324-AY226340(Bacteria); AY164429:AY164455 (Bacteria); AY226377-AY226381(Archaea); AY547867-AY548016 (Bacteria); DQ453257-DQ453476 (Bacteria and Archaea)	730
<i>Yakimov et al, 2014</i>	Kryos (gradient)	full-length RT-PCR	KJ922395-KJ922487 (Bacteria and Archaea)	67
<i>Daffonchino et al, 2006</i>	Bannock (gradient)	full length 16S gene	AM157647:AM157656 (Bacteria); AY547745:AY547866 (Bacteria) ; DQ289238:DQ289401 (Bacteria)	290
<i>Pachiadaki et al, 2014</i>	Thetis	partial 16S from RNA-seq metatranscriptome	n/a	None
<i>Yakimov et al, 2007</i>	L'Atalante (gradient)	full length RT-PCR	DQ453160:DQ453256 (Bacteria and Archaea); DQ453461:DQ453476	105
<i>La Cono et al, 2011</i>	Thetis (gradient)	full length RT-PCR	HQ658706:HQ658735	28
<i>Ngugi et al, 2015</i>	Atlantis II Deep (interface), Kebrit Deep (interface), Discovery Deep (interface), Erba Deep (interface), Nereus Deep (interface)	V3-V6 region; 454 Pyrosequencing; full-length 16S gene	SRP034153 (Pyrosequencing); KF954222:KF954277 (Archaea) (Sanger)	Data request pending
<i>Wang et al, 2011</i>	Atlantis II Deep (brine)	partial 16S from 454 metagenome	n/a	Data request pending
<i>Wang et al, 2013</i>	Atlantis II Deep (brine), Discovery (brine)	Assigning taxonomy to ORFs in 454 metagenome	n/a	None
<i>Guan et al, 2015</i>	Atlantis II Deep (interface), Kebrit Deep (interface), Discovery Deep (interface), Erba Deep (interface), Nereus Deep (interface)	full length 16S gene	KJ881441:KJ882283 (Archaea); KM018335:KM019141 (Bacteria); KP083299:KP083370 (Bacteria)	879
<i>Bougouffa et al, 2013</i>	Atlantis II Deep (gradient), Discovery Deep (interface and brine)	V5-V6; 454 Pyrosequencing	SRA052277	Data request pending

Table III. Available sequence data from other brine pools in the Mediterranean and Red Sea

3 *Results*

3.1 *Whole bacterial community*

Taxonomic classifications at the class-level for all bacterial sequences are shown in Figure 2. Both Alpha- and Gammaproteobacterial sequence abundance decrease dramatically along the chemocline (2150 m - 2210 m), whereas “AB16”-affiliated sequences (a class-level designation in the phylum Marinimicrobia/SAR406) increases in abundance along the same interval. Sequences recovered from the brine pool (2240-2390 m) show an entirely different bacterial community compared to the overlying water column and Orca Basin’s diffuse brine-seawater interface.

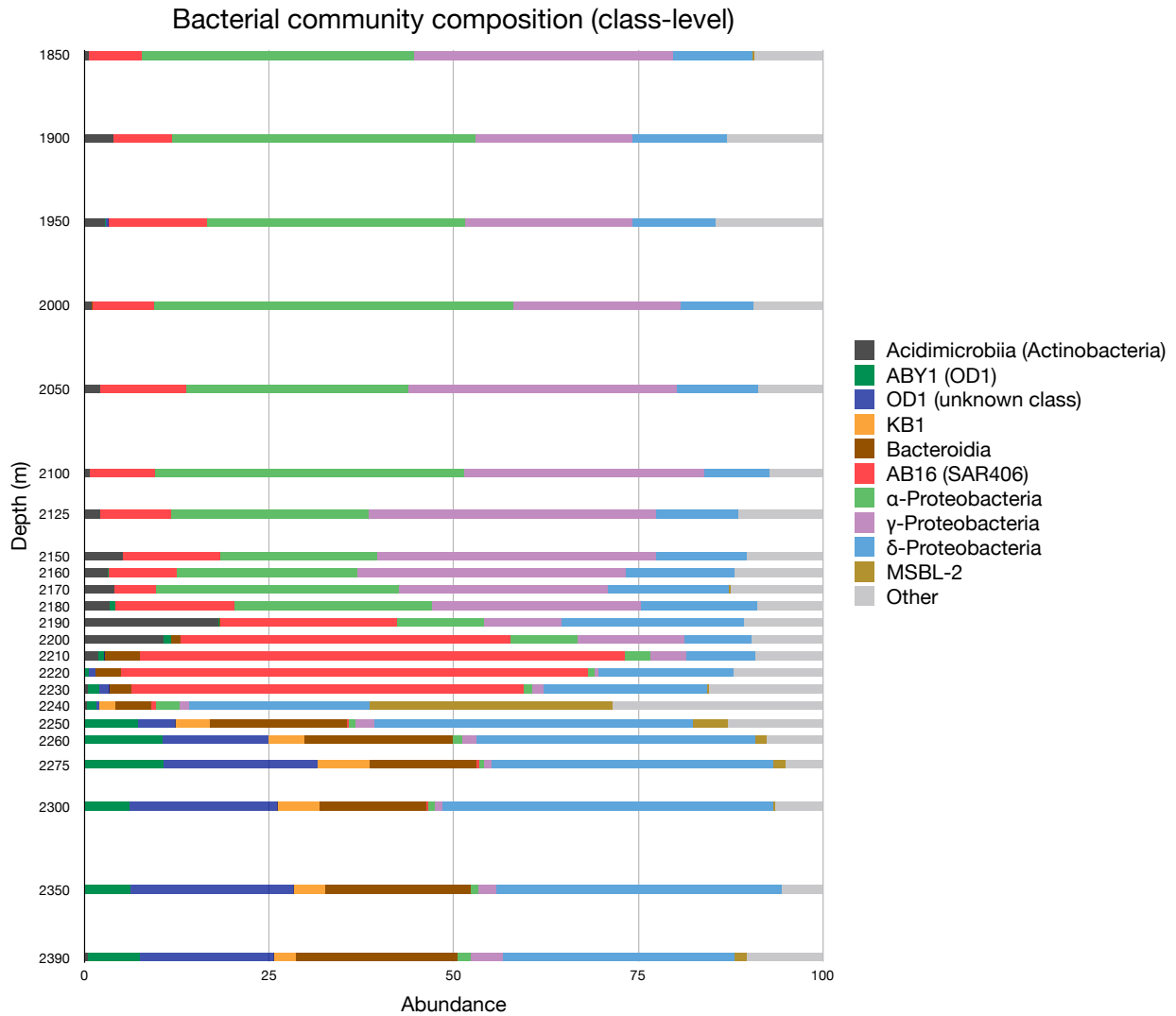


Figure 2. Class-level bacterial community composition for Orca Basin. Abundance of sequences in the dataset is shown on the x-axis; depth (in meters) below sea surface is shown on the y-axis.

3.2 *a*-diversity

The three measures of diversity within sample are shown in Figure 3. The number of OTUs is shown in the first panel and is lowest at 2350m and 2275m, both with 45 observed OTUs. The highest number of OTUs was detected at 2160m, with 175

distinct OTUs. Sequences were assigned to the same OTU if they showed a minimum of 97% sequence identify.

The ACE index is a way of estimating “richness” of microbial communities (number of OTUs) using rare taxa in a given dataset. The average number of estimated OTUs per sample is 185 ± 88 (standard deviation) compared to the 107 ± 43 OTUs actually observed in the dataset. The highest estimated richness is at 2160m (water column) with an ACE estimation of 364 OTUs (175 OTUs were actually observed). The lowest richness was estimated to be at 2390 m (bottom of the brine pool) with an ACE index of 71 predicted OTUs (56 actual observed).

Another way of quantifying α -diversity is to take relative frequencies into account- “evenness” (richness only takes presence/absence into account). The Shannon Diversity Index takes both evenness and richness into account, and reveals a clear pattern along the Orca Basin chemocline: The highest diversity occurs in the water column at 1950 m. The lowest diversity occurs at the halo- and redox cline at 2220m, and increases slightly below the interface and into the brine pool.

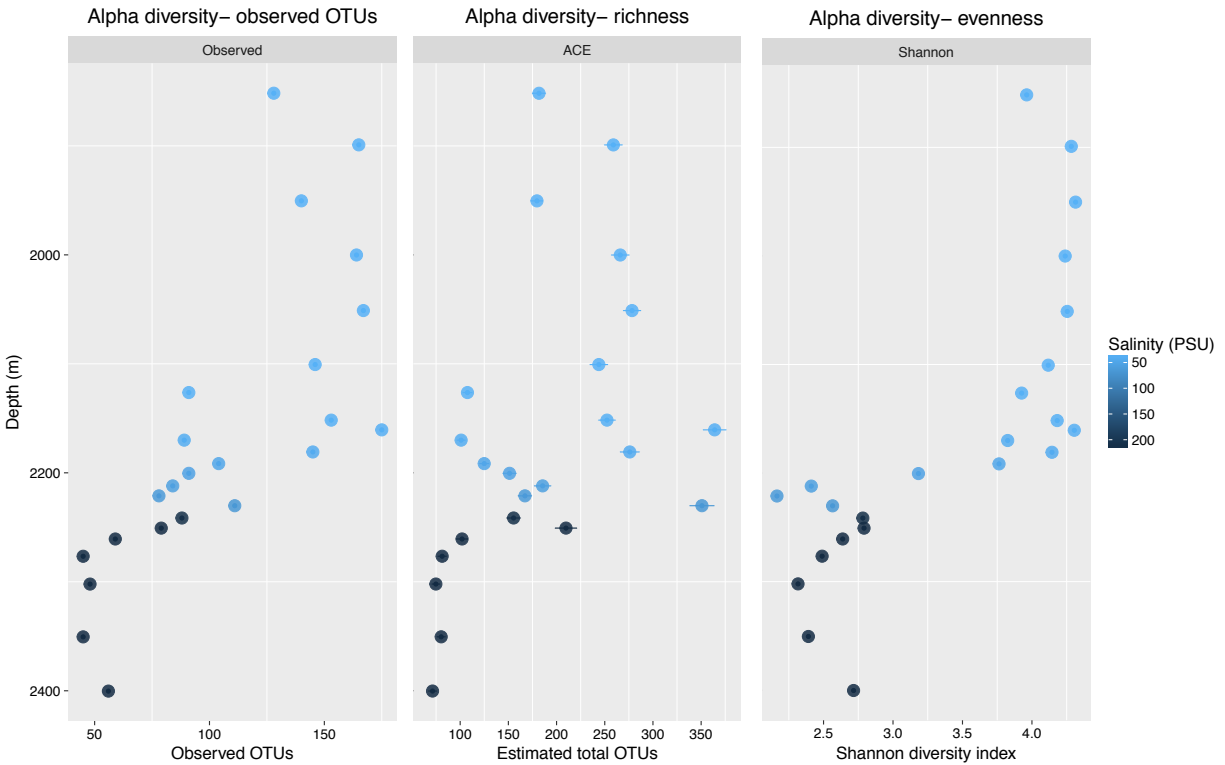


Figure 3. Measures of alpha-diversity in the Orca Basin chemocline. Three diversity metrics are shown- observed OTUs, ACE index, and the Shannon index (see text for description). Depth increases along the y-axis whereas the diversity metrics are shown on the x-axis. The color of the dot corresponds to the salinity for that sample with increasing salinity being denoted by darkening of the marker.

3.3 β -diversity

Six principle coordinate-analyses were done on the whole community dataset (Figure 4). The three distance matrices (Weighted UniFrac, Unweighted UniFrac, and Bray-Curtis Dissimilarity) all yielded more or less the same pattern on the rarefied dataset. All three groups (water column, interface, brine pool) form distinct clusters on a Cartesian plane. Transition communities were detected at 2190 m, 2200 m, and 2240 m.

Weighted UniFrac takes abundance into account, instead of just presence/absence (see Methods for details). Therefore, it better accounts for the low diversity in interface samples and is a better representation of the similarities and dissimilarities of the different bacterial communities. The variation within the dataset is primarily explained by Axis 1 (62.3% for the rarefied dataset; 63.3% for the unrarefied). Because the components in a PCoA are calculated using non-linear functions of the original variations (as opposed to linear functions in PCA- principle components analysis), it is not possible to directly translate an axis to a physical, environmental variable.

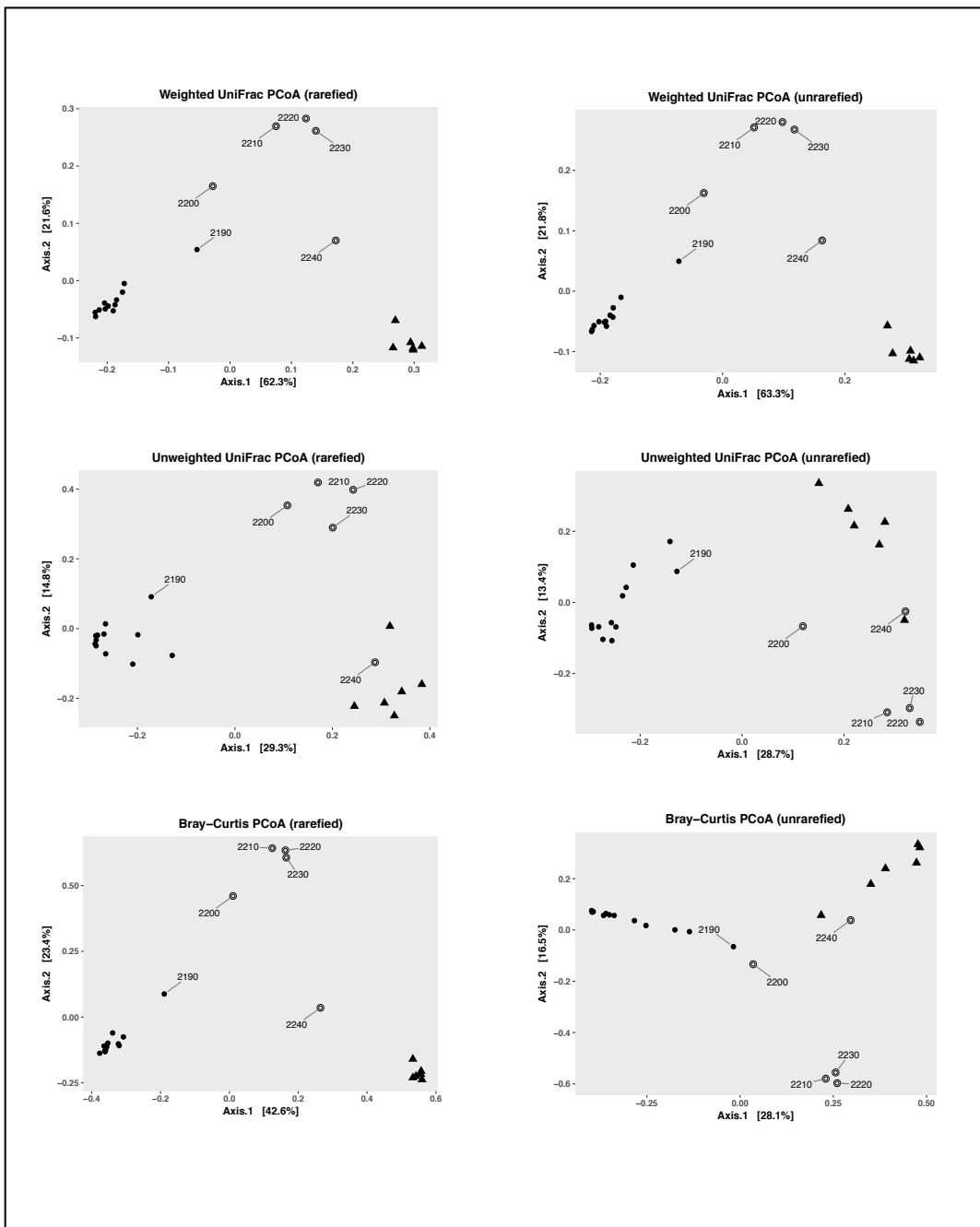


Figure 4. Principle Coordinate analyses for the rarefied and unrarefied datasets. Three different distance metrics are shown (Weighted UniFrac, Unweighted UniFrac, and Bray-Curtis Dissimilarity)

3.4 Examination of specific clades

3.4.1 Marinimicrobia (SAR406, Marine Group A)

Marinimicrobia (formerly known as SAR406 and Marine Group A) is a bacterial phylum lacking any cultured representatives.^{65,66} The abundance and distribution of Marinimicrobia sequences is shown in Figure 5. Overall, the phylum is represented by approximately 10% of the sequences in the water column; it is extremely enriched at the interface (~65% of the total community) and completely absent in the brine pool. The dominant order-level lineage within the Marinimicrobia, Arctic96B-7, is found in the brine pool interface and in the water column, the latter habitat also contains a small community of ZA3648c, another order-level lineage.

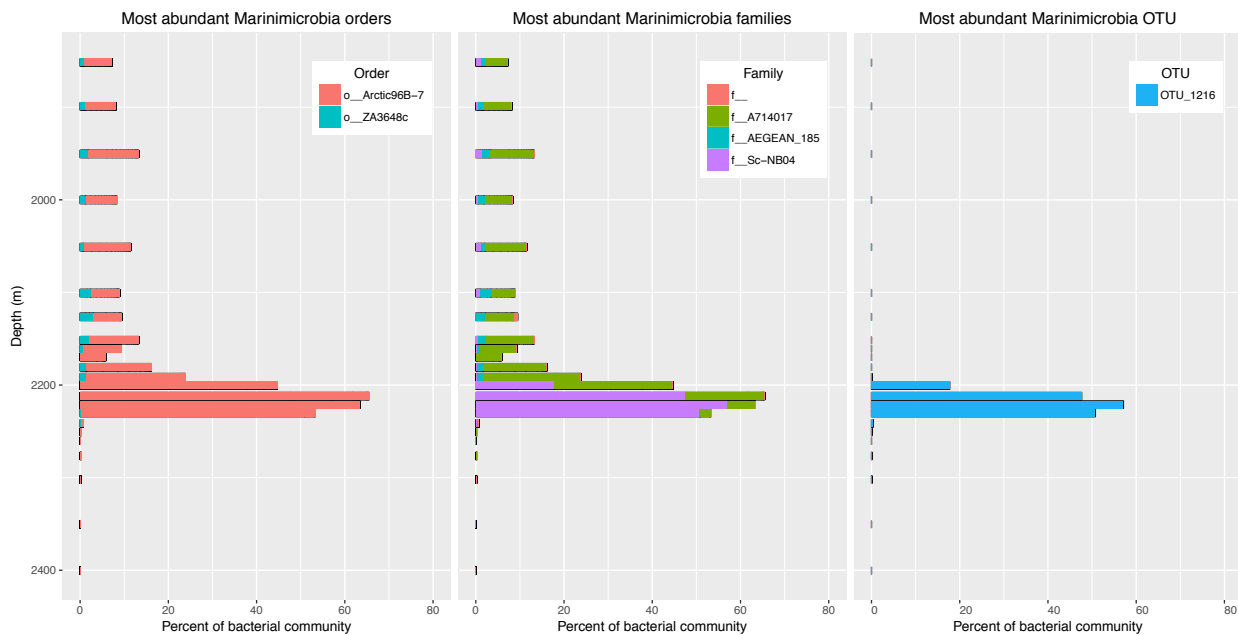


Figure 5. Distribution of Marinimicrobia (SAR406) along the Orca Basin halocline at three different taxonomic resolutions. Sequence abundance (x-axis) is plotted in percent of the total bacterial community sequence dataset

Within the order-level lineage Arctic96B-7, there are two predominant family-level lineages: A714017 and Sc-NB04 with the former being far more abundant above

the interface and the later being nearly absent in all samples other than those from the interface⁵². Interestingly, a single OTU (defined at 0.97 similarity) within Sc-NB04 accounts for 58% of the total bacterial sequences at 2210m (Figure 5). Below the interface (2220m) this OTU disappears along with the rest of the Marinimicrobial sequences.

Phylogenetic placement of this dominant Marinimicrobial OTU (“denovo1216”) is shown in Figure 6. A maximum-likelihood tree shows a close clustering with Marinimicrobia from DHABs in the Mediterranean and Red Seas as well as oxygen minimum zones (OMZs) in the Red Sea and the North Pacific. A very tight clustering was observed by site (i.e. all Nitinat Lake sequences formed a clade) and branches were therefore collapsed for clarity.

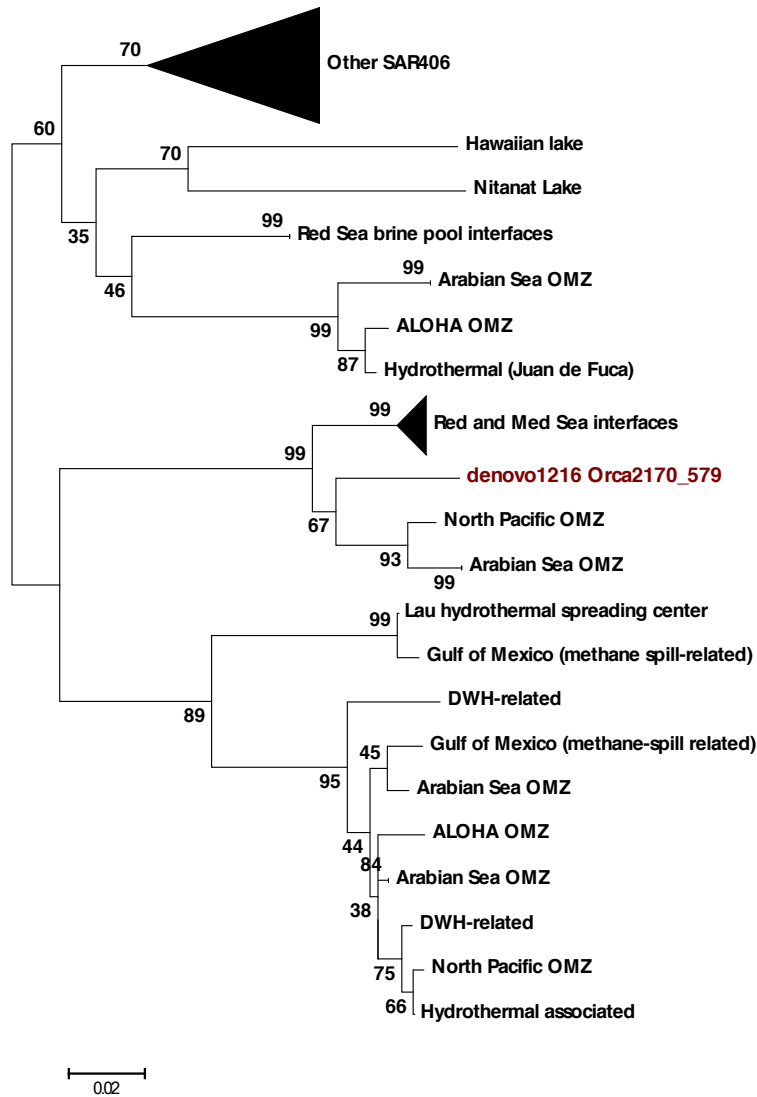


Figure 6. Maximum-Likelihood tree constructed for *denovo1216* from the Orca Basin interface. Values shown are for 100 bootstrap replicates with scores less than 35 not shown. Tightly clustered branches are collapsed for clarity.

3.4.2 Alphaproteobacteria

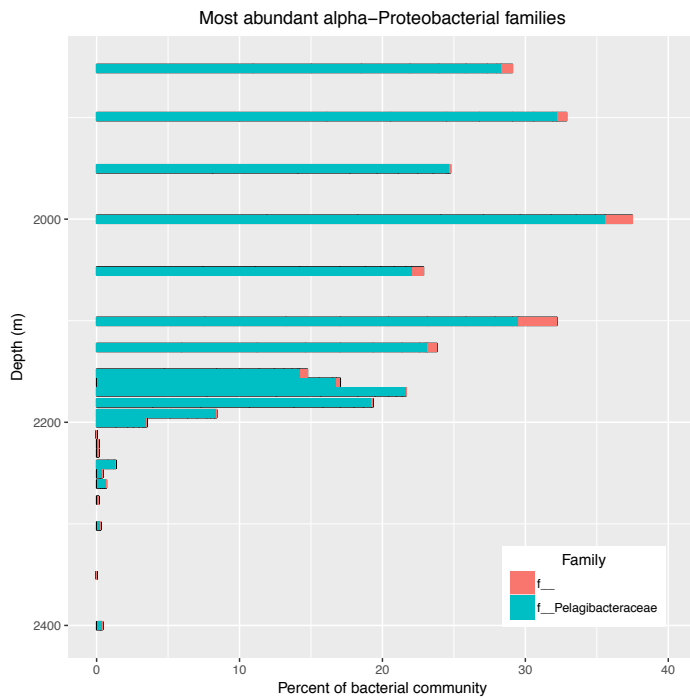


Figure 7. Distribution of Alphaproteobacteria along the Orca Basin halocline at order and family levels. Sequence abundance (x-axis) is plotted in percent of the total bacterial community sequence dataset.

The Alphaproteobacteria are almost exclusively affiliated with the family Pelagibacteraceae and show strong stratification in the Orca Basin. While alphaproteobacterial sequences in both the water column and the suboxic zone account for at up to forty percent of the total bacterial community dataset, they decrease to between one and two percent below the brine-seawater interface (Figure 7).

3.4.3 Gammaproteobacteria

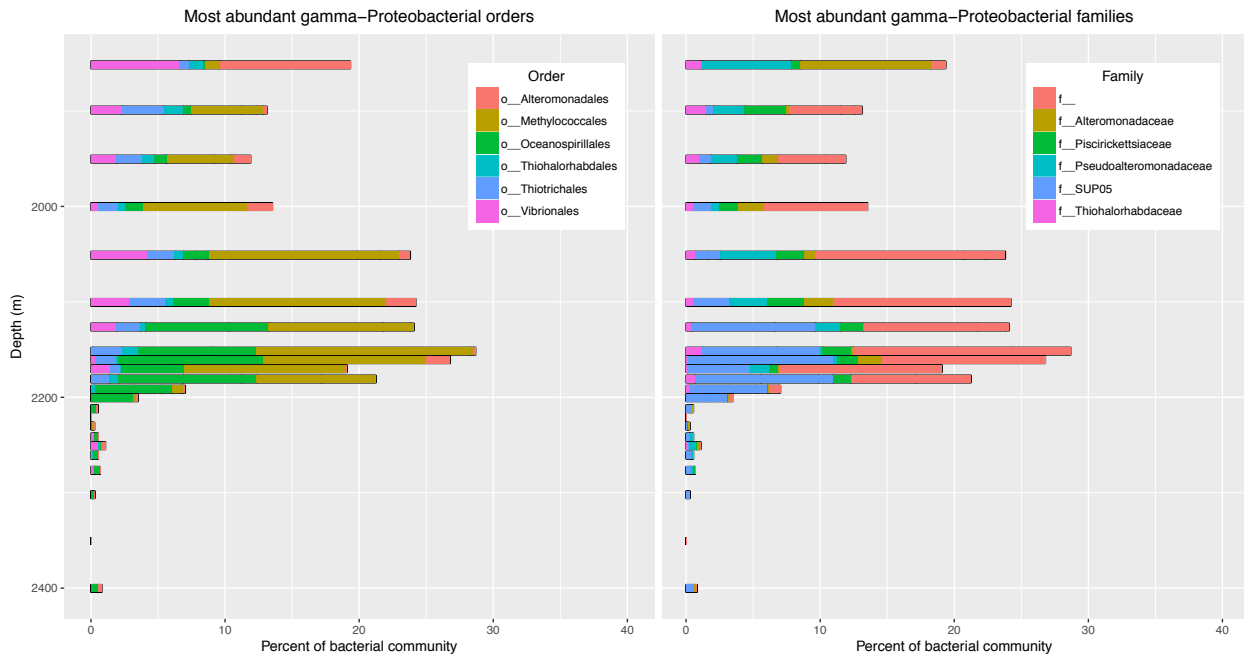


Figure 8. Distribution of Gammaproteobacteria along the Orca Basin halocline at order and family levels. Sequence abundance (x-axis) is plotted in percent of the total bacterial community sequence dataset.

The Gammaproteobacteria accounted for between ten and thirty percent of the total bacterial community in the water column. Most sequences were assigned to the order Methylococcales, but could not be further classified. Sequences affiliated with the families Piscirickettsiaceae (order Thiotrichales), the family-level SUP05 lineage (order Oceanospirillales), Pseudoalteromonadaceae, Alteromonadaceae (order Alteromonadales), and Thiohalorhabdaceae (order Thiohalorhabdadales) were recovered above the brine-seawater interface. Below the interface, the abundance of Gammaproteobacteria decreased to one to three percent of the total bacterial community (Figure 8).

3.4.4 Deltaproteobacteria

The sequences for the Deltaproteobacteria show a strongly stratified pattern in the Orca Basin chemocline. Figure 9 shows the relative abundance of Deltaproteobacteria with respect to the entire bacterial community. In the water column, this class makes up less than 10 percent of every sample, with the dominant family-level group being SAR324⁶⁷. In the suboxic zone, the Deltaproteobacteria increase in abundance (though relative proportions of the different families do not change). Once oxygen is completely depleted at 2200 m, the relative abundance of the deltaproteobacterial sequences decreases to three percent of the total community dataset. Below that depth, not only do the Deltaproteobacteria begin to increase in abundance again, but the community composition changes entirely; SAR324 is replaced by Desulfohalobiaceae and Desulfobulbaceae. A Weighted UniFrac-PCoA confirms the stratification (Figure 10) with the primary axis accounting for 71.6% of the observed variation in the Deltaproteobacteria.

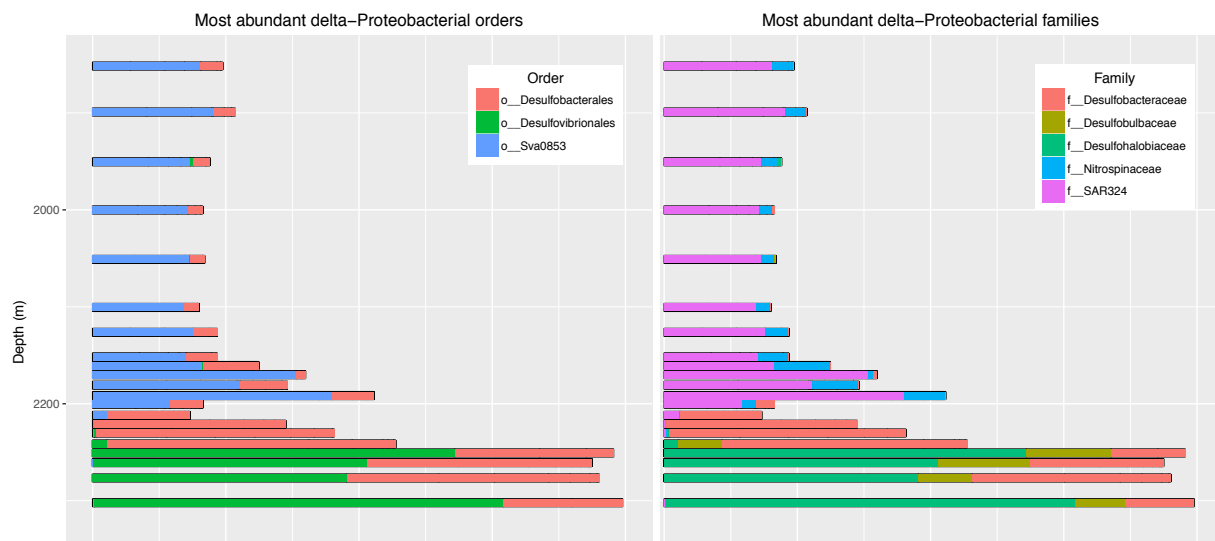


Figure 9. Distribution of Deltaproteobacteria along the Orca Basin halocline at order and family levels. Sequence abundance (x-axis) is plotted in percent of the total bacterial community sequence dataset.

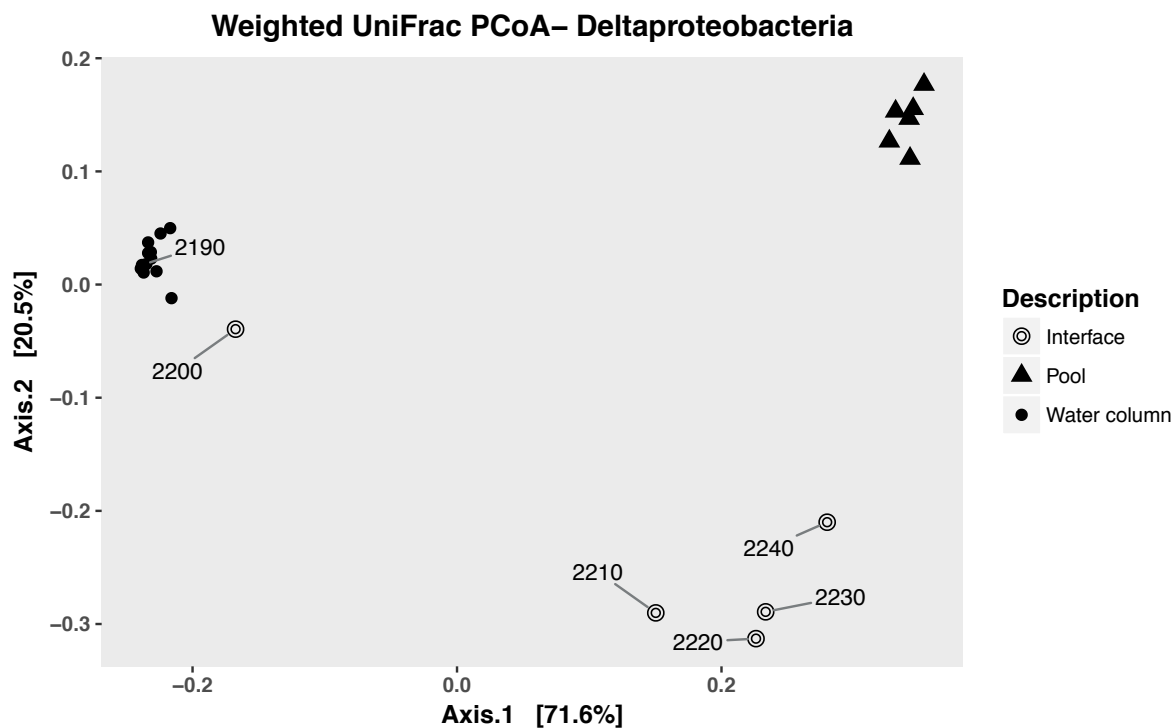


Figure 10. PCoA analysis on the Deltaproteobacterial community showing the clear stratification observed along the Orca Basin chemocline

3.4.5 Actinobacteria

The sequences of the Phylum Actinobacteria were affiliated with the orders Acidimicrobiales and Actinomycetales and accounted for less than five percent of all water-column sequences above the brine-seawater interface. However, at the interface, their proportion increased to 20 and 11 percent of the total community for 2190 and 2200 m, respectively (Figure 11). The sequences were not affiliated with any cultured Actinobacteria below the order level.

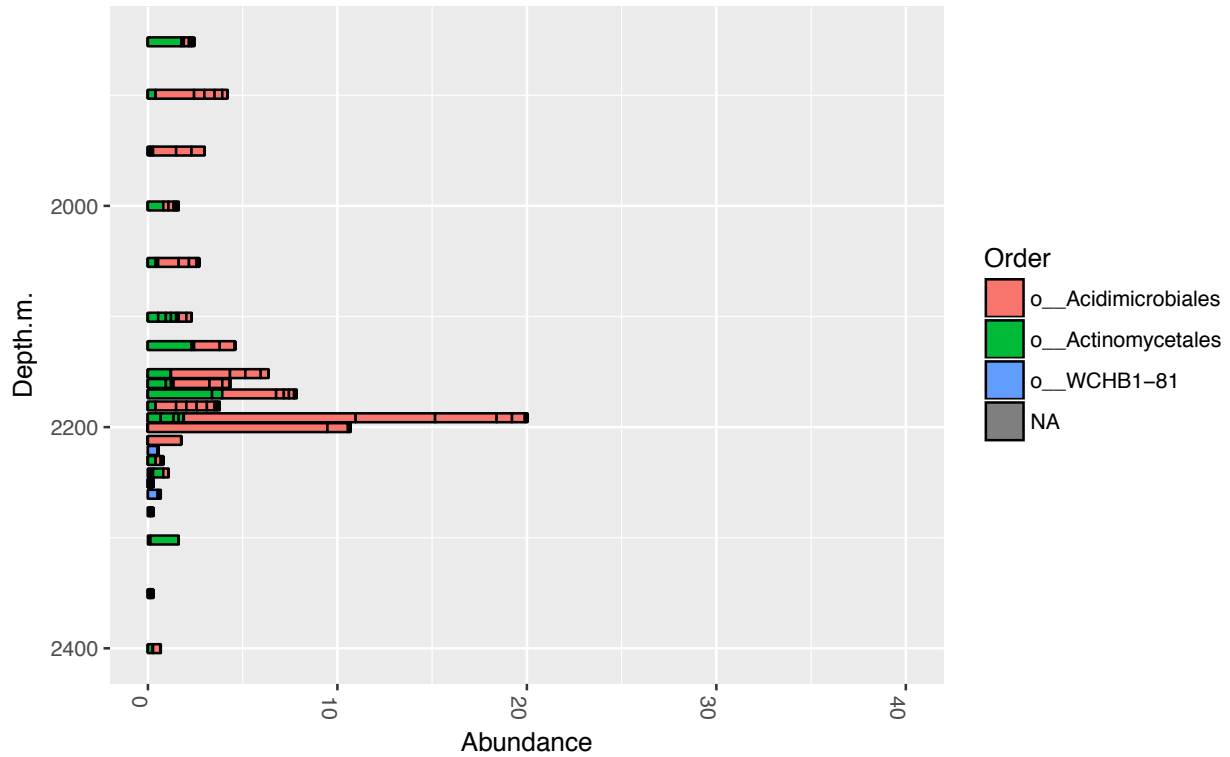


Figure 11. Distribution of Actinobacteria along the Orca Basin halocline at order level. Sequence abundance (x-axis) is plotted in percent of the total bacterial community sequence dataset.

3.4.6 MSBL2

The Mediterranean Sea Brine Lake group 2 (MSBL2) is a member of the phylum WWE1, which was recently renamed Cloacimonetes⁶⁸. Members of this class-level designation were only present in samples from the interface (as well as one at the bottom of the brine pool). Notably, members from this class made up 35% of the entire bacterial community at 2240m (brine-seawater interface) and decreased in abundance drastically after that.

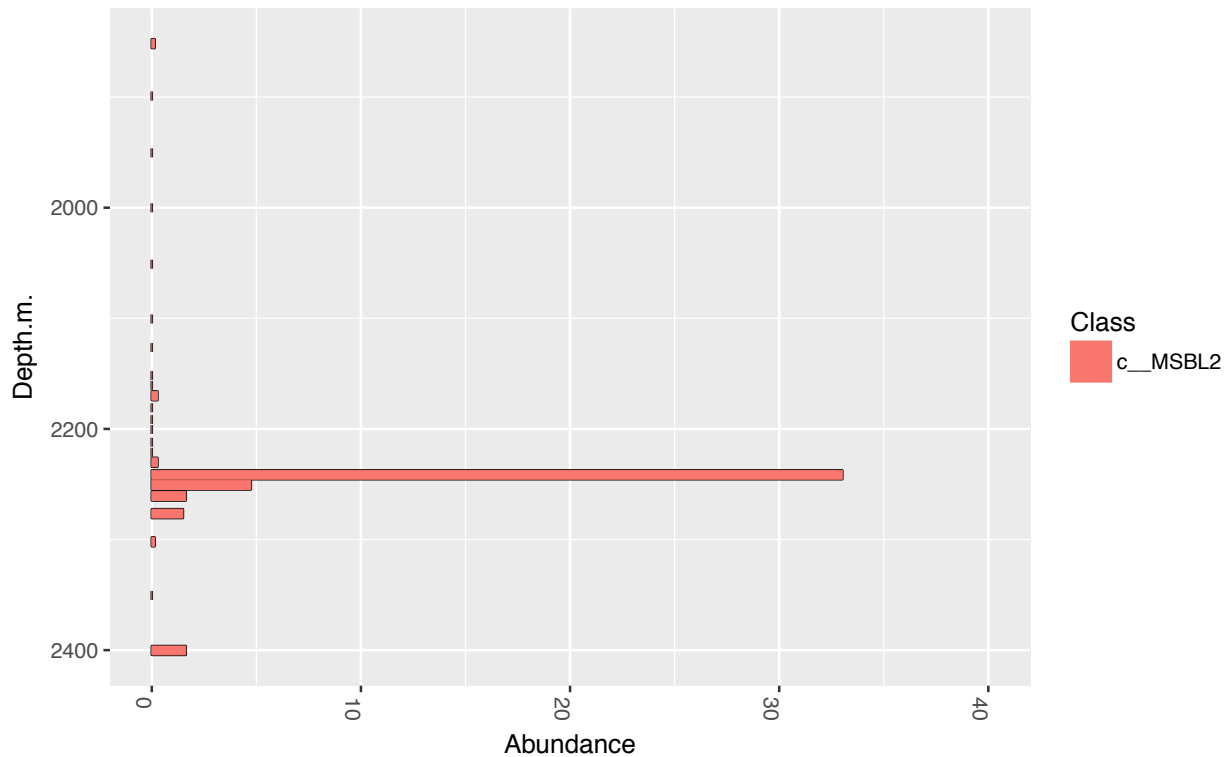


Figure 12. Distribution of WWE1 phylum along the Orca Basin halocline at class level. Sequence abundance (x-axis) is plotted in percent of the total bacterial community sequence dataset.

3.5 Mediterranean and Red Sea DHABs

Sequences downloaded from the GenBank database⁶⁴ were only annotated with “interface” or “brine”, so a finer-scale comparison of their origins within the halocline or brine (or affiliation with any environmental parameters, e.g. salinity, oxygen) was not possible. In order to compare Orca Basin’s interface community to the other DHAB interfaces, six different samples were used (2190m - 2240m). Class level comparisons are shown in Figure 13. (See Discussion for caveats regarding sequence comparisons between studies.)

Overall, Orca Basin samples 2190-2230 m had a bacterial community composition distinct from other DHAB interfaces (see Discussion). However, the bacterial community at 2240 m (the brine-seawater interface) shows greater compositional overlap by sharing a greater number of taxonomic groups with the other DHABs (Figure 13). All DHAB interfaces seem to have unique proportions of these groups (see Discussion).

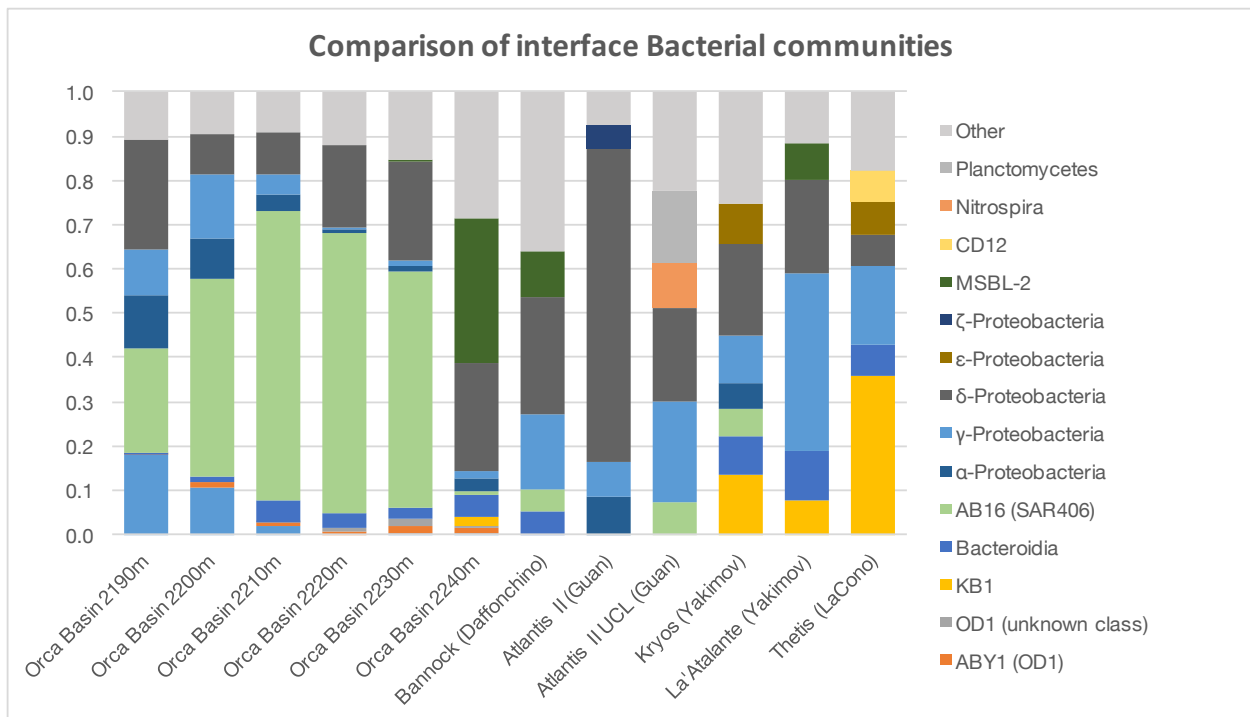


Figure 13. Comparison of the interface bacterial communities of the different DHABs.

The bacterial communities of the different brine pools appear to be much more similar to one another than the bacterial communities of the different brine-seawater interfaces. For comparisons among different brine pools, a representative sample from the Orca Basin brine pool was used, as the bacterial community is homogeneous below the brine-seawater interface (see Figure 14). Several differences and commonalities can be identified: OD1 sequences were present in the Orca Basin brine

at approximately 20 percent of the total community but were either not detected or in low abundance in other DHABs (e.g. 3.3% of community in Kebrit Deep).

Deltaproteobacteria were present in all datasets ranging from 12% of the total bacterial community in the brine of Discovery Basin, to 45% of the total bacterial community in Kebrit Deep. Gammaproteobacteria accounted for the smallest percentage of the total bacterial sequence dataset [2%] in Orca Basin, and a greater proportion in all other brine pools (7% in Erba to 40% in Discovery Deep)^{42,69}.

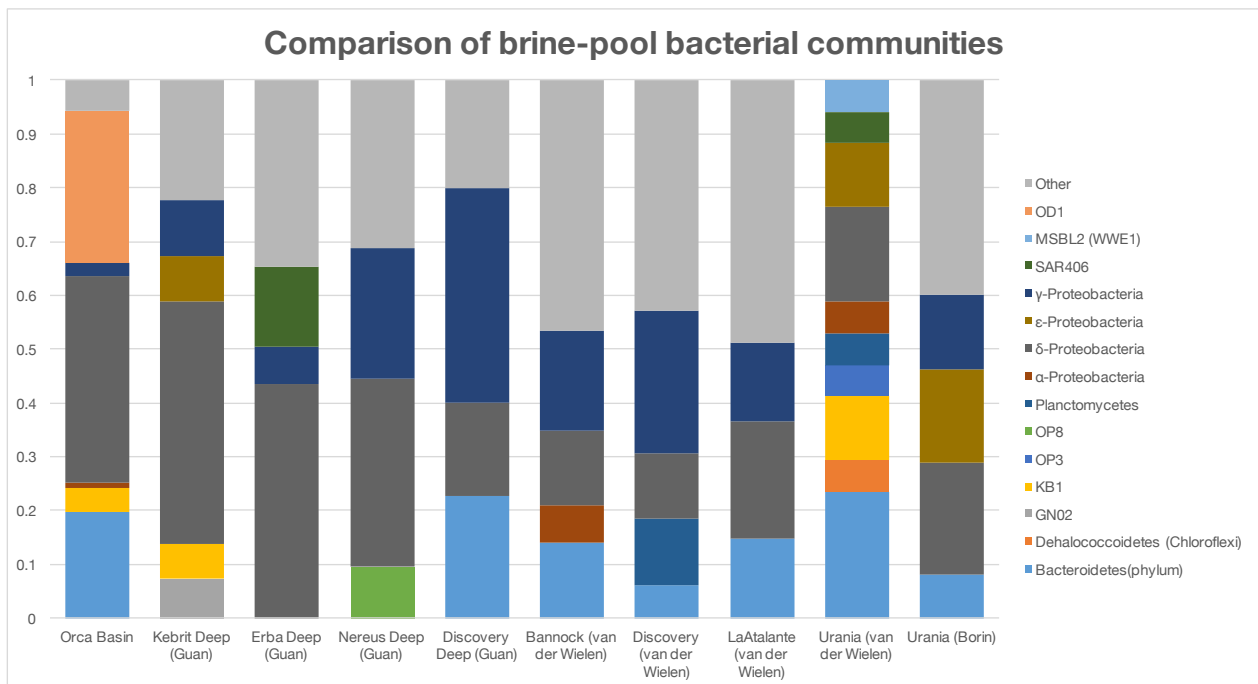


Figure 14. Comparison of bacterial communities in of different brine pools. Relative sequence abundance is plotted on the y-axis.

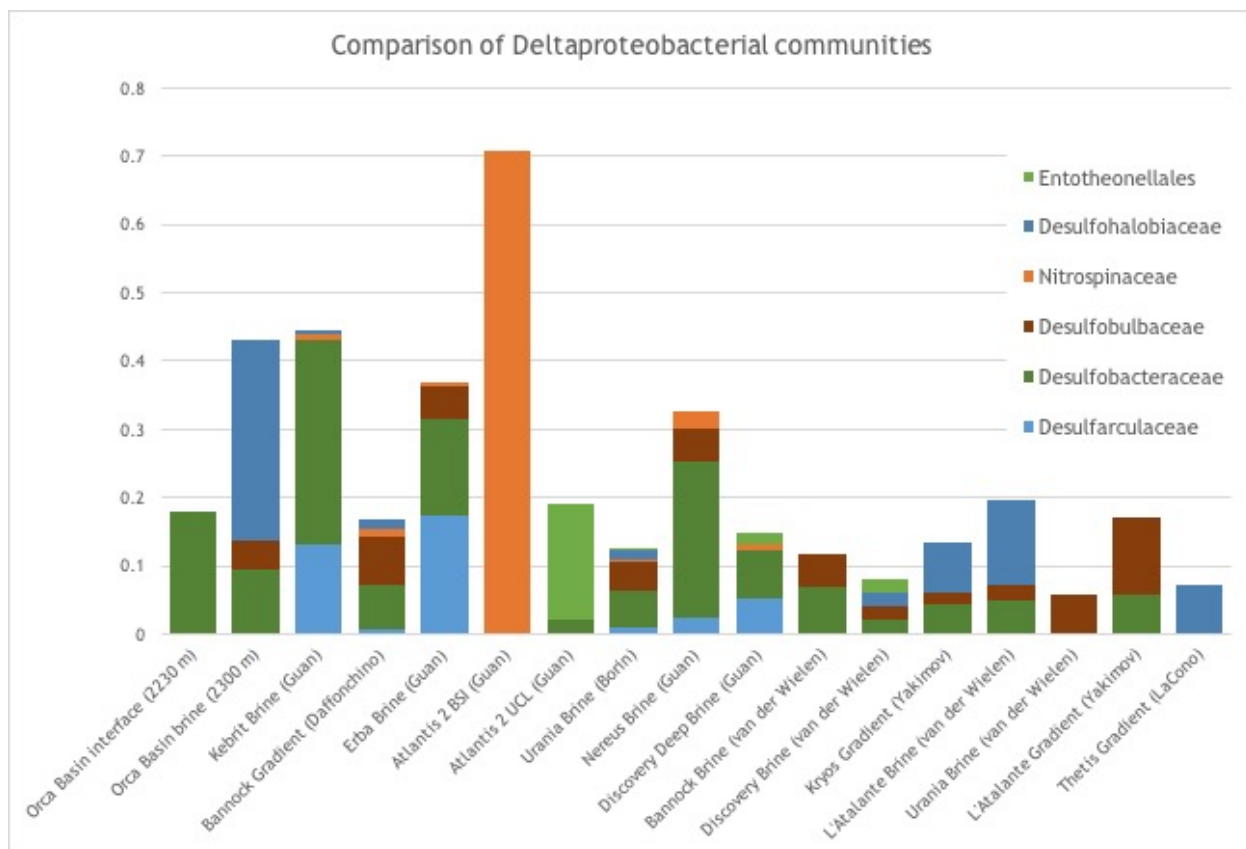


Figure 15. Comparison of the Deltaproteobacteria in the different interfaces and gradients. Sequence abundance (x-axis) is plotted in percent of the total bacterial community sequence dataset.

In Orca Basin, all Deltaproteobacterial groups, except for Desulfobacteraceae, were only present in one environment (i.e. seawater, interface, or brine pool). SAR324 was confined to the water column, *Desulfococcus* (a genus within the Desulfobacteraceae) to the interface, and Desulfohalobiaceae and Desulfobulbaceae were only seen in the brine pool. Members of the Desulfobacteraceae were present in both the brine pool and the interface.

In comparing these observations to other brine pools, few patterns emerge (Figure 15). The Desulfobacteraceae are present in all samples- pool and interface- except for the interface of Atlantis II Deep. This group was initially absent from Urania Basin in the 16S dataset from van der Wielen⁶⁹ but sequences from this group accounted for five percent of the total bacterial sequences in a subsequent study³⁰.

Desulfobulbaceae were not confined to brine pools in other studies, but were detected in the interfaces of the Bannock and Kryos Basins^{10,69}. Sequences from this group were detected in all brine pools except for Discovery, Kebrit Deep and the upper convective layer (UCL) of the Atlantis II Deep. Members of the Desulfohalobiaceae were only detected in brine pools (but not all brine pools) in addition to the Kryos and Bannock interfaces. Members of the genus *Desulfococcus* were frequently detected in brine pools (Discovery Deep, Erba Deep, and Nereus Deep), but were confined to the interface in Orca Basin.

4 Discussion

4.1 Sulfur cycling in the Orca Basin chemocline

The water column above the Orca Basin interface has a significant population of SAR324- a family level designation in the class Deltaproteobacteria. At 2190 m, SAR324 sequences account for approx. 18% of the total bacterial dataset. This abundance is similar to a 2011 survey from Station ALOHA (A Long-term Oligotrophic Habitat Assessment) and the South Atlantic, where SAR324 cells accounted for 6-17% of all bacterial and archaeal cells⁷⁰ The metabolic potential of SAR324 has only recently been elucidated using a combination of single-cell sequencing⁷⁰ and genome assembly⁷¹.

SAR324 has shown the potential to carry out sulfur-oxidation: metagenomic bins and single-cell genomes have shown the presence of *aprA* genes, which encodes for APS (adenosine-5'-phosphosulfate) reductase. However, this enzyme is common in both sulfate-reducing bacteria as well as sulfur-oxidizing bacteria⁷². Several phylogenetically distinguishable forms of *aprA* exist, but only genes from Clades I and II were found in SAR324 genomes; Group II forms of *aprA* are exclusively found in sulfur-oxidizing bacteria (SOB)⁷³. Furthermore, genes encoding reverse-type dissimilatory sulfite-reductase (*rdsrA*) were found, lending further credence to SAR324's ability to carry out dissimilatory sulfur oxidation. Studies of Guaymas Basin

have also shown SAR324 to express the same genes with respect to sulfur metabolism, while having the potential for many other sulfur-based metabolisms⁷¹.

At the Orca Basin interface, the most dominant OTU (otu1216; 58% of all bacterial sequences at 2210m) is affiliated with the Marinimicrobia order Arctic96B-7 and is given the family-level designation Sc-NB04⁵². While Marinimicrobia currently have no cultured representatives, recent genomes assembled from metagenomic datasets as well as metatranscriptomic analyses have revealed that at least some members of this phylum respire on elemental sulfur (S^0) or polysulfides (S_n^{2-}), producing (S^{2-}) as a product⁷⁴⁻⁷⁶. Marinimicrobia have been implicated in the marine sulfur cycle when fosmids affiliated with the group SHBH391 contained genes homologous to *psrA* (polysulfide reductase)^{74,77}. Interestingly, subsequent studies based on genome reconstruction and metatranscriptomics have confirmed these findings, however no genes for *psrA* have been found in members of the subgroup Arctic96B-7^{75,76}, the most dominant family-level lineage in the Orca Basin interface.

Specific genes may be missing because reconstructed genomes are not complete. While the Arctic96B-7 genome was estimated to be 94% complete in the Bertagnolli et al. study, 14.1% of the genes contained in the bin were suspected to be contaminants⁷⁶. Thrash et al, 2017 were able to form two distinct bins affiliated with Arctic96B-7, which were 73.6 and 21.3% complete⁷⁵. On the other hand, the absence of particular genes may indicate genuine metabolic differences. Interestingly, genes encoding cytoplasmic nitrate reductase (*narG*) were detected in the Arctic96B-7 genomes in these studies^{75,76} suggesting a replacement for sulfur reduction in for this member of the Marinimicrobia.

The brine pool has a significant population of Deltaproteobacteria (30-40%) belonging to three families: Desulfobacteraceae [including the genus *Desulfococcus*], Desulfohalobiaceae, and Desulfobulbaceae. All three of these groups are known to be obligate anaerobes, respiring with sulfate, sulfite, or thiosulfate, all of which are reduced to sulfide⁷⁸⁻⁸⁰. Previous questions have been raised over the lack of sulfide in the Orca Basin brine: does its absence indicate an absence of sulfate reduction or is the sulfide reacting with Orca Basin's abundant pool of Fe(II) to form pyrite^{81,82}? At the redoxcline, sulfide can be partially re-oxidized to sulfur or polysulfides, which are subsequently reduced by Marinimicrobia. While isotopic models and comparisons to other brines have provided evidence that sulfate reduction is occurring in Orca Basin⁸², this study identifies the potentially responsible microorganisms.

4.2 Carbon metabolism in the Orca Basin chemocline

Swan et al detected *cbbL/M* (the gene encoding the large subunit of RuBisCO) in 47% of SAR324 genomes⁷⁰. Ribulose-1,5-bisphosphate carboxylase/oxygenase (RuBisCO) is a critical enzyme in the Calvin-Benson-Bassham (CBB) cycle- one of the most widespread mechanisms of carbon fixation. Microautoradiography coupled to CARD-FISH (catalyzed auto-reporter deposition- fluorescent in situ hybridization) as well as transcriptomic evidence confirmed the expression of this gene at Station ALOHA⁷⁰. Therefore, these mesopelagic bacteria may play a role in global carbon assimilation; some Orca Basin populations of SAR324 may participate in this role in the "dark oceans" of the northern Gulf of Mexico. SAR324 has also been shown to actively transcribe particulate methane monooxygenase (pMMO) for aerobic methane

oxidation, which could potentially be fueled by the diffusive methane flux from the Orca Basin brine below⁴⁶.

However, SAR324 has also been implicated in heterotrophic processes such as alkane, fatty-acid, amino acid, sugar, oligopeptide, and alcohol degradation^{70,71}. In the interface, members of the Marinimicrobia are likely to be degrading the organic carbon that is trapped in the density interface. The high amount of particulate matter would likely favor a heterotrophic metabolism. In particular, the reconstructed genomes and metagenomes of Arctic96B-7 contain genes that strongly indicate a heterotrophic lifestyle. One metagenome-derived bin for this group (94% complete) contained 37 different peptidase-encoding genes, as well as the complete machinery for flagellum assembly, and all genes for the TCA cycle⁷⁶. The published genomic data for this group has only shown an ability to use nitrate as a terminal electron acceptor⁷⁵, in contrast to other members of the Marinimicrobia where the genomic evidence indicates sulfur reduction. It is possible that the abundance of organic matter coupled to the high energy yield of nitrate reduction^{83,84} could account for the abundance of OTU1216 in Orca Basin's interface.

Desulfococcus is capable of using a wide variety of carbon compounds as both carbon and electron sources for dissimilatory sulfate reduction. In culture, some compounds utilized by this genus include: monocarboxylic acid (up to C16), pyruvate, lactate, formate, and alcohols; these are all oxidized completely to CO₂⁸⁵. Recent stable isotope incubations have implicated members of *Desulfococcus* in playing a key role in dodecane oxidation coupled to sulfate reduction⁸⁶. While dodecane at Orca

Basin has yet to be measured, the brine is known to have elevated concentrations of hydrocarbons >C₁⁴⁶.

All Deltaproteobacterial lineages detected in the brine pool have shown the ability oxidize a variety of organic compounds to acetate (or to CO₂, in the case of *Desulfococcus*) by coupling these reactions to sulfate respiration⁷⁸⁻⁸⁰. These lineages have also shown the ability to ferment organic compounds in culture⁷⁸⁻⁸⁰ and while this is a certainly a possibility, the energetically expensive adaptations required by hypersaline conditions may impose bioenergetic constraints on the competitiveness of this metabolic regime⁸⁷.

Recent work has been done on the remaining lineages in the brine pool indicating that they could play a significant role in carbon cycling in Orca Basin. For example, OD1 microbes are thought to carry out fermentative metabolism⁸⁸, which could play a role in providing the lactate, acetate, and pyruvate which the Deltaproteobacteria in the brine pool are oxidizing by sulfate reduction.

4.3 Comparison of Orca Basin to other DHABs

While methodological differences and the changes in sequencing technology preclude any sort of meaningful statistical comparison between DHABs^{51,89,90}, some general trends can be observed. The first is that the Orca Basin interface is host to a truly unique microbial community. Marinimicrobial sequences are detected in the Upper Convective Layer (UCL) of Atlantis II Deep, in the interface of Kryos Basin, and in the interface of Bannock Basin. However, no brine pool has an interface community that is as dominated by this clade as Orca Basin, specifically between 2190-2340m. This result perhaps suggests that the spatially extended interface at Orca Basin,

where salinity and oxygen content change over this depth interval, provides a unique habitat for these microorganisms that other DHABs do not. Although Marinimicrobia thrive in suboxic conditions such as oxygen minimum zones (OMZs)^{65,91}, this group has not previously been seen in similarly high abundance^{74,75,92}.

Deltaproteobacteria are the only group observed in every interface sample analyzed here. The ubiquity of this group in the marine environment is not surprising as seawater provides a readily available source of sulfate, which is used by many members of this group as a terminal electron acceptor. Once the oxygen and nitrate are depleted, sulfate becomes the next readily accessible electron acceptor for respiration. However, it should also be noted that aerobic and nitrate respiration has been documented in several sulfate-reducing Deltaproteobacteria⁹³⁻⁹⁶, making them especially suited for an oxic-anoxic interface. The abundance of Deltaproteobacteria may also be due to the presence of halophily and halotolerance among many bacteria in this group^{27,78,80,85,97,98}. Furthermore, the Deltaproteobacteria seen at the DHAB interfaces can utilize a wide variety of substrates (e.g. alcohols and low-molecular weight organic acids)^{78,80,85}, allowing them to thrive in these environments.

Brine pool bacterial communities appear to be much more similar to one another than interface communities. Nearly all samples have a community dominated by potential sulfate-reducing bacteria (Deltaproteobacteria), while Gammaproteobacteria are detected in smaller proportion. However, unlike the Deltaproteobacteria, Gammaproteobacterial sequences represent a wider diversity of mutually coexisting order-level lineages (see Appendix). Some of the more prominent groups (e.g. Halomonadaceae) are known to tolerate a wide range of salinities and

have a variety of metabolisms⁹⁹, so speculation into their role in these pools is not possible.

But these Gammaproteobacteria could also represent the preserved DNA^{29,100} of particle-associated populations from the interface that sink into the brine; their apparent diversity could indicate that a wide variety of Gammaproteobacteria is preserved equally well. For some Deltaproteobacteria, the same argument may apply, but since extreme halophiles are known, some may still be active.

REFERENCES

1. Charnock, H. Anomalous Bottom Water in the Red Sea. *Nature* **203**, 591-591 (1964).
2. Warren, J. K. *Evaporite sedimentology*. 1-298 (Prentice Hall, 1989). doi:10.1016/0037-0738(92)90121-7
3. Stoffers, P. & Kühn, R. in *Initial Reports of the Deep Sea Drilling Project*, **23** **23**, 821-847 (U.S. Government Printing Office, 1974).
4. Coleman, R. G. *Geologic Background of the Red Sea. Initial Reports of the Deep Sea Drilling Project* **23**, (U.S. Government Printing Office, 1974).
5. Adams, C. G., Benson, R. H., Kidd, R. B., Ryan, W. B. F. & Wright, R. C. The Messinian salinity crisis and evidence of late Miocene eustatic changes in the world ocean. *Nature* **269**, 383-386 (1977).
6. Duggen, S., Hoernle, K., van den Bogaard, P., Rüpke, L. & Morgan, J. P. Deep roots of the Messinian salinity crisis. *Nature* **422**, 602-606 (2003).
7. Krijgsman, W., Hilgen, F. J., Raffi, I., Sierro, F. J. & Wilson, D. S. Chronology, causes and progression of the Messinian salinity crisis. *Nature* **400**, 652-655 (1999).
8. Cita, M. B. Exhumation of Messinian evaporites in the deep-sea and creation of deep anoxic brine-filled collapsed basins. *Sedimentary Geology* **188-189**, 357-378 (2006).
9. Lerche, I. & Petersen, K. *Salt and Sediment Dynamics*. (CRC Press, 1995).
10. Yakimov, M. M. *et al.* Microbial community of the deep-sea brine Lake Kryos seawater-brine interface is active below the chaotropy limit of life as revealed by recovery of mRNA. *Environ Microbiol* **17**, 364-382 (2015).
11. Miller, A. R. *et al.* Hot brines and recent iron deposits in deeps of the Red Sea. *Geochimica et Cosmochimica Acta* **30**, 341-359 (1966).
12. Craig, H. in *Hot Brines and Recent Heavy Metal Deposits in the Red Sea* 208-242 (Springer Berlin Heidelberg, 1969). doi:10.1007/978-3-662-28603-6_22
13. Anschutz, P. *et al.* Hydrographic changes during 20 years in the brine-filled basins of the Red Sea. *Deep Sea Research Part I: Oceanographic Research Papers* **46**, 1779-1792 (1999).

14. Winckler, G. *et al.* Constraints on origin and evolution of Red Sea brines from helium and argon isotopes. *Earth and Planetary Science Letters* **184**, 671-683 (2001).
15. Shokes, R. F., Trabant, P. K., Presley, B. J. & Reid, D. F. Anoxic, Hypersaline Basin in the Northern Gulf of Mexico. *Science* **196**, 1443-1446 (1977).
16. Salvador, A. Late Triassic-Jurassic paleogeography and origin of Gulf of Mexico basin. *AAPG Bulletin* **71**, 419-451 (1987).
17. Peel, F. J., Hudec, M. R., Norton, I. O. & Jackson, M. P. A. Jurassic evolution of the Gulf of Mexico Salt Basin. *AAPG Bulletin* **97**, 1683-1710 (2013).
18. Pilcher, R. & Blumstein, R. Brine volume and salt dissolution rates in Orca Basin, northeast Gulf of Mexico. *AAPG Bulletin* **91**, 823-833 (2007).
19. Shah, S. R., Joye, S. B., Brandes, J. A. & McNichol, A. P. Carbon isotopic evidence for microbial control of carbon supply to Orca Basin at the seawater-brine interface. *Biogeosciences* **10**, 3175-3183 (2013).
20. Oren, A. Life at high salt concentrations, intracellular KCl concentrations, and acidic proteomes. *Front. Microbiol.* **4**, 315 (2013).
21. Yakimov, M. M., La Cono, V. & Denaro, R. Primary producing prokaryotic communities of brine, interface and seawater above the halocline of deep anoxic lake L'Atalante, Eastern Mediterranean Sea. *The ISME ...* (2007).
22. La Cono, V. *et al.* Unveiling microbial life in new deep-sea hypersaline Lake Thetis. Part I: Prokaryotes and environmental settings. *Environ Microbiol* **13**, 2250-2268 (2011).
23. Pachiadaki, M. G., Yakimov, M. M., LaCono, V., Leadbetter, E. & Edgcomb, V. Unveiling microbial activities along the halocline of Thetis, a deep-sea hypersaline anoxic basin. *The ISME Journal* **8**, 2478-2489 (2014).
24. Sackett, W. M. *et al.* A carbon inventory for Orca Basin brines and sediments. *Earth and Planetary Science Letters* **44**, 73-81 (1979).
25. Yakimov, M. M., Giuliano, L., Cappello, S., Denaro, R. & Golyshin, P. N. Microbial Community of a Hydrothermal Mud Vent Underneath the Deep-Sea Anoxic Brine Lake Urania (Eastern Mediterranean). *Orig Life Evol Biosph* **37**, 177-188 (2006).
26. Yakimov, M. M. *et al.* Microbial life in the *Lake Medee*, the largest deep-

- sea salt-saturated formation. *Sci. Rep.* **3**, srep03554 (2013).
27. van der Wielen, P. W. J. J. & Heijs, S. K. Sulfate-reducing prokaryotic communities in two deep hypersaline anoxic basins in the Eastern Mediterranean deep sea. *Environ Microbiol* **9**, 1335-1340 (2007).
 28. Borin, S. *et al.* Anammox bacterial populations in deep marine hypersaline gradient systems. *Extremophiles* **17**, 289-299 (2013).
 29. Borin, S. *et al.* DNA is preserved and maintains transforming potential after contact with brines of the deep anoxic hypersaline lakes of the Eastern Mediterranean Sea. *Saline Systems* **2008 4:1 4**, 1 (2008).
 30. Borin, S. *et al.* Sulfur cycling and methanogenesis primarily drive microbial colonization of the highly sulfidic Urania deep hypersaline basin. *Proc Natl Acad Sci USA* **106**, 9151-9156 (2009).
 31. Daffonchio, D. *et al.* Stratified prokaryote network in the oxic-anoxic transition of a deep-sea halocline. *Nature* **440**, 203-207 (2006).
 32. Ferrer, M. *et al.* Unveiling microbial life in the new deep-sea hypersaline Lake Thetis. Part II: a metagenomic study. *Environ Microbiol* **14**, 268-281 (2012).
 33. Kormas, K. A. *et al.* Inter-comparison of the potentially active prokaryotic communities in the halocline sediments of Mediterranean deep-sea hypersaline basins. *Extremophiles* **19**, 949-960 (2015).
 34. Ngugi, D. K. *et al.* Comparative genomics reveals adaptations of a halotolerant thaumarchaeon in the interfaces of brine pools in the Red Sea. *The ISME Journal* **9**, 396-411 (2015).
 35. Ngugi, D. K., Blom, J., Stepanauskas, R. & Stingl, U. Diversification and niche adaptations of Nitrospina-like bacteria in the polyextreme interfaces of Red Sea brines. *The ISME Journal* **10**, 1383-1399 (2015).
 36. Eder, W., Jahnke, L. L. & Schmidt, M. Microbial Diversity of the Brine-Seawater Interface of the Kebrit Deep, Red Sea, Studied via 16S rRNA Gene Sequences and Cultivation Methods. *Applied and Environmental Microbiology* **67**, 3077-3085 (2001).
 37. Schmidt, M. *et al.* High-resolution methane profiles across anoxic brine-seawater boundaries in the Atlantis-II, Discovery, and Kebrit Deeps (Red Sea). *Chemical Geology* **200**, 359-375 (2003).
 38. Zhang, W. *et al.* Genomic and Transcriptomic Evidence for Carbohydrate

- Consumption among Microorganisms in a Cold Seep Brine Pool. *Front. Microbiol.* **7**, 533 (2016).
39. Eder, W., Schmidt, M., Koch, M., Garbe Schönberg, D. & Huber, R. Prokaryotic phylogenetic diversity and corresponding geochemical data of the brine-seawater interface of the Shaban Deep, Red Sea. *Environ Microbiol* **4**, 758-763 (2002).
 40. Wang, Y. *et al.* Autotrophic Microbe Metagenomes and Metabolic Pathways Differentiate Adjacent Red Sea Brine Pools. *Sci. Rep.* **3**, 1748 (2013).
 41. Wang, Y. *et al.* Hydrothermally generated aromatic compounds are consumed by bacteria colonizing in Atlantis II Deep of the Red Sea. *The ISME Journal* **5**, 1652-1659 (2011).
 42. Guan, Y., Hikmawan, T., Stingl, U., Antunes, A. & Ngugi, D. Diversity of methanogens and sulfate-reducing bacteria in the interfaces of five deep-sea anoxic brines of the Red Sea. *Research in Microbiology* **166**, 688-699 (2015).
 43. Bougouffa, S. *et al.* Distinctive Microbial Community Structure in Highly Stratified Deep-Sea Brine Water Columns. *Applied and Environmental Microbiology* **79**, 3425-3437 (2013).
 44. Dickins, H. D. & Van Vleet, E. S. Archaeobacterial activity in the Orca Basin determined by the isolation of characteristic isopranyl ether-linked lipids. *Deep Sea Research Part A. Oceanographic Research Papers* **39**, 521-536 (1992).
 45. Van Cappellen, P. *et al.* Biogeochemical Cycles of Manganese and Iron at the Oxidic-Anoxic Transition of a Stratified Marine Basin (Orca Basin, Gulf of Mexico). *Environ. Sci. Technol.* **32**, 2931-2939 (1998).
 46. Wiesenburg, D. A., Brooks, J. M., Brooks, J. M., Bernard, B. B. & Bernard, B. B. Biogenic hydrocarbon gases and sulfate reduction in the Orca Basin brine. *Geochimica et Cosmochimica Acta* **49**, 2069-2080 (1985).
 47. Zhuang, G.-C. *et al.* Multiple evidence for methylotrophic methanogenesis as the dominant methanogenic pathway in hypersaline sediments from the Orca Basin, Gulf of Mexico. *Geochimica et Cosmochimica Acta* **187**, 1-20 (2016).
 48. Wang, Y. & Qian, P.-Y. Conservative Fragments in Bacterial 16S rRNA Genes and Primer Design for 16S Ribosomal DNA Amplicons in Metagenomic Studies. *PLoS ONE* **4**, e7401 (2009).

49. John, J. S. SeqPrep.
50. Edgar, R. C. Search and clustering orders of magnitude faster than BLAST. *Bioinformatics* **26**, 2460-2461 (2010).
51. Caporaso, J. G. *et al.* QIIME allows analysis of high-throughput community sequencing data. *Nat Meth* **7**, 335-336 (2010).
52. Cole, J. R. *et al.* The Ribosomal Database Project: improved alignments and new tools for rRNA analysis. *Nucleic Acids Research* **37**, D141-D145 (2009).
53. Kopylova, E., Noé, L. & Touzet, H. SortMeRNA: fast and accurate filtering of ribosomal RNAs in metatranscriptomic data. *Bioinformatics* **28**, 3211-3217 (2012).
54. Caporaso, J. G. *et al.* PyNAST: a flexible tool for aligning sequences to a template alignment. *Bioinformatics* **26**, 266-267 (2010).
55. Haas, B. J. *et al.* Chimeric 16S rRNA sequence formation and detection in Sanger and 454-pyrosequenced PCR amplicons. *Genome Res.* **21**, 494-504 (2011).
56. Price, M. N., Dehal, P. S. & Arkin, A. P. FastTree 2 - Approximately Maximum-Likelihood Trees for Large Alignments. *PLoS ONE* **5**, e9490 (2010).
57. McMurdie, P. J. & Holmes, S. phyloseq: An R Package for Reproducible Interactive Analysis and Graphics of Microbiome Census Data. *PLoS ONE* **8**, e61217 (2013).
58. McMurdie, P. J. & Holmes, S. Waste Not, Want Not: Why Rarefying Microbiome Data Is Inadmissible. *PLoS Comput Biol* **10**, e1003531 (2014).
59. Chao, A. & Lee, S.-M. Estimating the Number of Classes via Sample Coverage. *Journal of the American Statistical Association* **87**, 210-217 (1992).
60. Hill, M. O. Diversity and Evenness: A Unifying Notation and Its Consequences. *Ecology* **54**, 427-432 (1973).
61. Lozupone, C. A., Hamady, M., Kelley, S. T. & Knight, R. Quantitative and Qualitative β Diversity Measures Lead to Different Insights into Factors That Structure Microbial Communities. *Applied and Environmental Microbiology* **73**, 1576-1585 (2007).

62. Lozupone, C. & Knight, R. UniFrac: a New Phylogenetic Method for Comparing Microbial Communities. *Applied and Environmental Microbiology* **71**, 8228-8235 (2005).
63. Bray, J. R. & Curtis, J. T. An Ordination of the Upland Forest Communities of Southern Wisconsin. *Ecological Monographs* **27**, 325-349 (1957).
64. Benson, D. A. *et al.* GenBank. *Nucleic Acids Research* **41**, D36-D42 (2013).
65. Fuhrman, J. A., McCallum, K. & Davis, A. A. Phylogenetic diversity of subsurface marine microbial communities from the Atlantic and Pacific Oceans. *Applied and Environmental Microbiology* **59**, 1294-1302 (1993).
66. Gordon, D. A. & Giovannoni, S. J. Detection of stratified microbial populations related to Chlorobium and Fibrobacter species in the Atlantic and Pacific oceans. *Applied and Environmental Microbiology* **62**, 1171-1177 (1996).
67. Wright, T. D., Vergin, K. L., Boyd, P. W. & Giovannoni, S. J. A novel delta-subdivision proteobacterial lineage from the lower ocean surface layer. *Applied and Environmental Microbiology* **63**, 1441-1448 (1997).
68. Rinke, C. *et al.* Insights into the phylogeny and coding potential of microbial dark matter. *Nature* **499**, 431-437 (2013).
69. van der Wielen, P. W. J. J. *et al.* The Enigma of Prokaryotic Life in Deep Hypersaline Anoxic Basins. *Science* **307**, 121-123 (2005).
70. Swan, B. K., Martinez-Garcia, M. & Preston, C. M. Potential for chemolithoautotrophy among ubiquitous bacteria lineages in the dark ocean. *Science* **333**, 1296-1300 (2011).
71. Sheik, C. S., Jain, S. & Dick, G. J. Metabolic flexibility of enigmatic SAR324 revealed through metagenomics and metatranscriptomics. *Environ Microbiol* **16**, 304-317 (2013).
72. Bertrand, J.-C. *et al.* *Environmental Microbiology: Fundamentals and Applications*. (2015). doi:10.1007/978-94-017-9118-2
73. Meyer, B. & Kuever, J. Molecular Analysis of the Diversity of Sulfate-Reducing and Sulfur-Oxidizing Prokaryotes in the Environment, Using *aprA* as Functional Marker Gene. *Applied and Environmental Microbiology* **73**, 7664-7679 (2007).
74. Wright, J. J. *et al.* Genomic properties of Marine Group A bacteria indicate a role in the marine sulfur cycle. *The ISME Journal* **8**, ismej2013152-468

- (2013).
75. Thrash, J. C. *et al.* Metabolic Roles of Uncultivated Bacterioplankton Lineages in the Northern Gulf of Mexico 'Dead Zone'. *mBio* **8**, e01017-17 (2017).
 76. Bertagnolli, A. D., Padilla, C. C., Glass, J. B., Thamdrup, B. & Stewart, F. J. Metabolic potential and in situ activity of marine Marinimicrobia bacteria in an anoxic water column. *Environ Microbiol* **7**, 256 (2017).
 77. Krafft, T. *et al.* Cloning and nucleotide sequence of the *pst A* gene of *Wolinella succinogenes* polysulphide reductase. *The FEBS Journal* **206**, 503-510 (1992).
 78. Kuever, J. in *The Prokaryotes* 45-73 (Springer Berlin Heidelberg, 2014). doi:10.1007/978-3-642-39044-9_266
 79. Kuever, J. in *The Prokaryotes* 87-95 (Springer Berlin Heidelberg, 2014). doi:10.1007/978-3-642-39044-9_311
 80. Kuever, J. in *The Prokaryotes* 75-86 (Springer Berlin Heidelberg, 2014). doi:10.1007/978-3-642-39044-9_267
 81. Sheu, D.-D., Presley, B. J. & Presley, B. J. Formation of Hematite in the Euxinic Orca Basin, Northern Gulf of Mexico. **69**, 309-321 (1986).
 82. Sheu, D. D. The anoxic Orca Basin (Gulf of Mexico): geochemistry of brines and sediments. *Reviews in Aquatic Sciences* **2**, 491-507 (1990).
 83. Zumft, W. G. Cell biology and molecular basis of denitrification. **61**, 533-616 (1997).
 84. Shapleigh, D. J. P. in (eds. Rosenberg, E., DeLong, E. F., Lory, S., Stackebrandt, E. & Thompson, F.) 405-425 (Springer Berlin Heidelberg, 2013).
 85. Kuever, J., Rainey, F. A. & Widdel, F. *Desulfococcus*. **8**, 1-5 (John Wiley & Sons, Ltd, 2015).
 86. Kleindienst, S. *et al.* Diverse sulfate-reducing bacteria of the *Desulfosarcina/Desulfococcus* clade are the key alkane degraders at marine seeps. *The ISME Journal* **8**, 2029-2044 (2014).
 87. Oren, A. Thermodynamic limits to microbial life at high salt concentrations. *Environ Microbiol* **13**, 1908-1923 (2011).

88. Wrighton, K. C. *et al.* Fermentation, Hydrogen, and Sulfur Metabolism in Multiple Uncultivated Bacterial Phyla. *Science* **337**, 1661-1665 (2012).
89. Ramette, A. Multivariate analyses in microbial ecology. *FEMS Microbiol Ecol* **62**, 142-160 (2007).
90. Lozupone, C. A. & Knight, R. Species divergence and the measurement of microbial diversity. *FEMS Microbiol Rev* **32**, 557-578 (2008).
91. Stevens, H. & Ulloa, O. Bacterial diversity in the oxygen minimum zone of the eastern tropical South Pacific. *Environ Microbiol* **10**, 1244-1259 (2008).
92. Allers, E. *et al.* Diversity and population structure of Marine Group A bacteria in the Northeast subarctic Pacific Ocean. *The ISME Journal* **7**, 256-268 (2012).
93. Dilling, W. & Cypionka, H. Aerobic respiration in sulfate-reducing bacteria. *FEMS Microbiol Lett* **71**, 123-127 (1990).
94. Cypionka, H. Oxygen Respiration by *Desulfovibrio* Species. *Annu. Rev. Microbiol.* **54**, 827-848 (2000).
95. Marschall, C., Frenzel, P. & Cypionka, H. Influence of oxygen on sulfate reduction and growth of sulfate-reducing bacteria. *Arch Microbiol* **159**, 168-173 (1993).
96. Dannenberg, S., Kroder, M., Dilling, W. & Cypionka, H. Oxidation of H₂, organic compounds and inorganic sulfur compounds coupled to reduction of O₂ or nitrate by sulfate-reducing bacteria. *Arch Microbiol* **158**, 93-99 (1992).
97. Häusler, S. *et al.* Sulfate reduction and sulfide oxidation in extremely steep salinity gradients formed by freshwater springs emerging into the Dead Sea. *FEMS Microbiol Ecol* **90**, 956-969 (2014).
98. Jakobsen, T. F. *Desulfohalobium utahense* sp. nov., a moderately halophilic, sulfate-reducing bacterium isolated from Great Salt Lake. *International Journal of Systematic and Evolutionary Microbiology* **56**, 2063-2069 (2006).
99. Arahal, D. R. & Ventosa, A. in *The Prokaryotes* 811-835 (Springer New York, 2006). doi:10.1007/0-387-30746-X_28
100. Corinaldesi, C., Tangherlini, M., Luna, G. M. & Dell'anno, A. Extracellular DNA can preserve the genetic signatures of present and past viral infection events in deep hypersaline anoxic basins. *Proceedings of the Royal Society*

B: Biological Sciences **281**, 20133299-20133299 (2014).